

# Rhyacian evolution of the eastern São Luís Craton: petrography, geochemistry and geochronology of the Rosário Suite

*Evolução riaciana no leste do Cráton São Luís:  
petrografia, geoquímica e geocronologia da Suíte Rosário*

Bruna Karine Correa Nogueira<sup>1\*</sup>, Paulo Sergio de Sousa Gorayeb<sup>1</sup>,  
Elton Luiz Dantas<sup>2</sup>, Rafael Estumano Leal<sup>1</sup>, Marco Antonio Galarza<sup>1</sup>

**ABSTRACT:** The São Luís Craton comprises an area between northeast Pará state and northwest Maranhão that exposes Paleoproterozoic granitic suites and meta-volcanosedimentary sequences. In the east of this geotectonic unit, about 70 km south of São Luís, there is a portion of the São Luís Craton, represented by the intrusive Rosario Suite (RS). This work is focused on rocks of this suite, including petrographic, lithochemical and geochronological studies to understand the crustal evolution of these granitoid rocks. The rock spectrum varies from tonalitic to granodioritic, quartz dioritic and granitic compositions, and there are partial structural and mineralogical changes related to deformation along transcurrent shear zones. The geochemical studies show granitic metaluminous compositions of the calc-alkaline series with I-type affinity typical of magmatic arc. Rare earth elements show marked fractionation and slight Eu positive or negative anomalies ( $\text{Eu/Eu}^* = 0.82$  to 1.1). Zircon U-Pb data provided consistent ages of  $2165 \pm 7$  Ma,  $2170 \pm 7$  Ma,  $2170 \pm 7$  Ma,  $2161 \pm 4$  Ma and  $2175 \pm 8$  Ma, dating emplacement of these granitoids as Paleoproterozoic (Rhyacian). Sm-Nd isotopic data provided model ages ( $T_{\text{DM}}$ ) of 2.21 to 2.31 Ga with positive values of  $\epsilon\text{Nd} +1.9$  to  $+3.2$  ( $t = 2.17$  Ga), indicating predominantly Rhyacian crustal sources for the parental magmas, similar to those ones found in other areas of the São Luís Craton. The data, integrated with published geological and geochronological information, indicate the occurrence of an important continental crust formation event in this area. The Paleoproterozoic evolution between 2.17 and 2.15 Ga is related to the Transamazonian orogeny. The granitoids of the Rosario Suite represent the main phase of continental arc magmatism that has continuity in other parts of the São Luís Craton and can be correlated with Rhyacian accretionary magmatism in the northwestern portion of the Amazonian Craton that amalgamated Archean terrains during the Transamazonian orogeny.

**KEYWORDS:** Rosário Suite; São Luís Craton; Petrology; U-Pb geochronology; Sm-Nd  $T_{\text{DM}}$ .

**RESUMO:** O Cráton São Luís compreende uma área entre o nordeste do estado do Pará e o noroeste do Maranhão que expõe suítes graníticas e sequências metavolcanosedimentares do Paleoproterozóico. No leste dessa unidade geotectônica, a cerca de 70 km ao sul da cidade de São Luís, há uma porção do Cráton São Luís representada pela Suíte Intrusiva Rosário. Este trabalho foi focado em rochas dessa suíte, incluindo estudos petrográficos, litioquímicos e geocronológicos para compreender a evolução crustal dessas rochas granitoides. O espectro de rochas varia de composições tonálticas, granodioríticas, quartzo dioríticas e graníticas, que mostram alterações estruturais e mineralógicas parciais relacionadas à deformação ao longo das zonas de cisalhamento transcorrentes. Os estudos geoquímicos demonstram a natureza granítica metaluminosa caracterizando a série calcioalcalina com afinidade de granitos tipo I, típicos de ambiente de arco magnático. Os elementos terras raras apresentam fracionamento acentuado e ligeiras anomalias de Eu positivas ou negativas ( $\text{Eu/Eu}^* = 0.82$  a 1.1). Datações pelo método U-Pb em zircão forneceram idades consistentes de  $2165 \pm 7$  Ma,  $2170 \pm 7$  Ma,  $2170 \pm 7$  Ma,  $2161 \pm 4$  Ma e  $2175 \pm 8$  Ma que representam a idade de cristalização dos zircões e de colocação desses granitoides no Paleoproterozóico (Riaciano). Os dados isotópicos Sm-Nd forneceram idades modelo ( $T_{\text{DM}}$ ) de 2,21 a 2,31 Ga, que são muito próximas às idades de cristalização, com valores positivos de  $\epsilon\text{Nd} = +1.9$  a  $+3.2$  ( $t = 2.17$  Ga), indicando fonte crustal dominanteamente do Riaciano para os magnas parentais, similares aos encontrados em outros domínios do Cráton São Luís. Os dados deste estudo, integrados às informações geológicas e geocronológicas da literatura, indicam a ocorrência de um importante evento de formação de crosta continental nessa área, por meio de múltiplo alojamento de plátanos graníticos da série calcioalcalina. A evolução paleoproterozóica entre 2,17 e 2,15 Ga está relacionada com a orogenia transamazônica, e os granitoides da Suíte Rosário representam a fase principal de acreção na evolução de um arco magnético continental juvenil, que tem continuidade para outras partes do Cráton São Luís e correlação com a porção noroeste do Cráton Amazônico, onde se têm registros de arcos magnéticos acrecionários riacianos que se amalgamaram em terrenos arqueanos, associados à orogenia transamazônica.

**PALAVRAS-CHAVE:** Suíte Rosário; Cráton São Luís; Petrologia; Geocronologia U-Pb; Sm-Nd  $T_{\text{DM}}$

<sup>1</sup>Programa de Pós-Graduação em Geologia e Geoquímica, Instituto de Geociências, Universidade Federal do Pará – UFPA, Belém (PA), Brazil.

<sup>2</sup>Instituto de Geociências, Universidade de Brasília – UnB, Brasília (DF), Brazil. E-mails: brunanogueira2611@gmail.com; gorayeb@ufpa.br; elton@unb.br; antogn@ufpa.br; rafael.leal@ig.ufpa.br

\*Corresponding author.

Manuscript ID: 20160114. Received in: 03/20/2016. Approved in: 05/09/2017.

## INTRODUCTION

In models of global supercontinent reconstruction, the São Luís Craton and the northeastern portion of the Amazonian Craton (to the east of the Guayana Shield) have been considered remnants of the West African Craton preserved in the northern South American Platform after the breakup of the Pangea Supercontinent (Hurley *et al.* 1967, Torquato & Cordani 1981, Lesquer *et al.* 1984, Brito Neves *et al.* 2000, Klein and Moura 2008).

On the African side, several studies based on structural, geochemical, geophysical and geochronological data demonstrate the existence of Archean and dominantly juvenile Paleoproterozoic crust (Abouchami *et al.* 1990, Boher *et al.* 1992, Gasquet *et al.* 2003). On the Brazilian side, the northern part of the Amazonian Craton and São Luís Craton have demonstrated geochronological and evolutionary similarities. In this part of the Amazonian Craton, the ancient continental crust stabilized in the Archean is bordered by meta-volcanosedimentary sequences (Rosa-Costa *et al.* 2006) and 2.02–2.25 Ga granitic terranes (Cordani *et al.* 1979, Cordani & Brito Neves 1982, Tassinari & Macambira 1999, Santos *et al.* 2000, Tassinari *et al.* 2000, Tassinari & Macambira 2004, Rosa-Costa *et al.* 2006).

The main outcrop area of the São Luís Craton crops out for some 100 km near the Atlantic coast. The rocks are discontinuously exposed in erosive or tectonic windows within the sedimentary cover (Gorayeb *et al.* 1999). The main lithological associations are meta-volcanosedimentary sequences and granitoids (Gorayeb *et al.* 1999, Klein *et al.* 2005b).

Despite recent advances in knowledge of the evolution of the São Luís Craton, systematic and more detailed studies are needed owing to the wide variety of the rocks of this tectonic unit, the difficulties of access, the restriction of outcrops and the extensive Phanerozoic cover.

The study area is located approximately 70 km south of São Luís, in Maranhão State, northeastern of Brazil, where the easternmost fragment of the craton is exposed as a set of granitic rocks named by Rodrigues *et al.* (1994) and Gorayeb *et al.* (1999) as the Rosário Suite (Fig. 1). The present work involves the study of a varied set of granitoid rocks included in the Rosario Suite, still little known from the cartographic, geochemical, geochronological and petrological point of view. In addition, the age range of magmatism is not well determined, the geochemical signature is not fully known, and it is unclear whether they represent juvenile crust or older reworked crust.

This research includes new data on granitoids of the Rosário Suite, particularly petrographic, geochemical, geochronological (LA-ICP-MS) and isotopic (Sm-Nd) data. Considering along available data in the literature, it allows us to discuss the crustal evolution of the suite, to make correlations with

granitoids of other portions of the São Luís Craton, and to contribute to the advancement of the evolutionary models.

## REGIONAL GEOLOGY CONTEXT

The São Luís Craton consists generally of three main Paleoproterozoic rock associations: a meta-volcanosedimentary succession, volcanic sequences and granitoids (Fig. 1). Older rocks ( $2240 \pm 5$  Ma) belong to the Aurizona Group, which comprises a meta-volcanosedimentary succession of schists, felsic and mafic meta-volcanic rocks, quartzites and meta-cherts.

The Tromáí Suite (2168 to 2,148 Ma, single zircon Pb-evaporation) (Klein & Moura 2001) is the most extensive igneous unit. It is formed of tonalite, trondhjemite, granodiorite and granite that belong to a juvenile calc-alkaline series related to an intra-oceanic island-arc to transitional setting (Klein & Moura 2001, Klein *et al.* 2008). Volcanic rocks with similar ages were included into the Serra do Jacaré and Rio Diamante units, with the chemical characteristics of a transitional arc in an active continental margin (Klein *et al.* 2009). The Rosilha volcanic unit is younger (2069 Ma) than the other two volcanic units (~2160 Ma), and has a post-orogenic tectonic setting (Klein *et al.* 2009).

Gorayeb *et al.* (1999) characterized the Rosário Suite as a set of composite tonalitic, granodioritic and granitic plutons with Paleoproterozoic ages (2.08–2.13 Ga). The rocks exhibit partial textural, structural and mineralogical transformations along transcurrent shear zones.

Other granitoids that have biotite and muscovite, peraluminous and S-type characteristics are represented by the Ourém, Japiim, Jonas, Tracuateua and Mirasselas bodies, aged 2.14 to 2.06 Ga (Palheta *et al.* 2009, Klein *et al.* 2012). The Negra Velha Granite (2056–2,076 Ma) consists of small granitic bodies intruded into the Tromáí Granitic Suite and associated with felsic volcanic and pyroclastic rocks of the same age (Klein *et al.* 2008, 2009). The Caxias Microtonalite, with age of  $2009 \pm 11$  Ma (Klein *et al.* 2014), represents the youngest magmatic plutonic activity of this cratonic area.

The Gurupi Belt is interpreted as a Neoproterozoic–early Cambrian orogen with NNW-SSE orientation, developed in the south-southwestern margin of the São Luís Craton (Almeida *et al.* 1976, Abreu *et al.* 1980 Costa 2000, Klein *et al.* 2005a, 2012). The belt and its reworked basement include rock units of varied nature and ages ranging from Archean to Eocambrian (Klein *et al.* 2005b, Palheta *et al.* 2009).

Several plutonic bodies are exposed as basement units of the Gurupi Belt and represent a variety of granitoid types emplaced at different times. They show zircon inheritance and chemical and isotopic features that imply participation in the magma

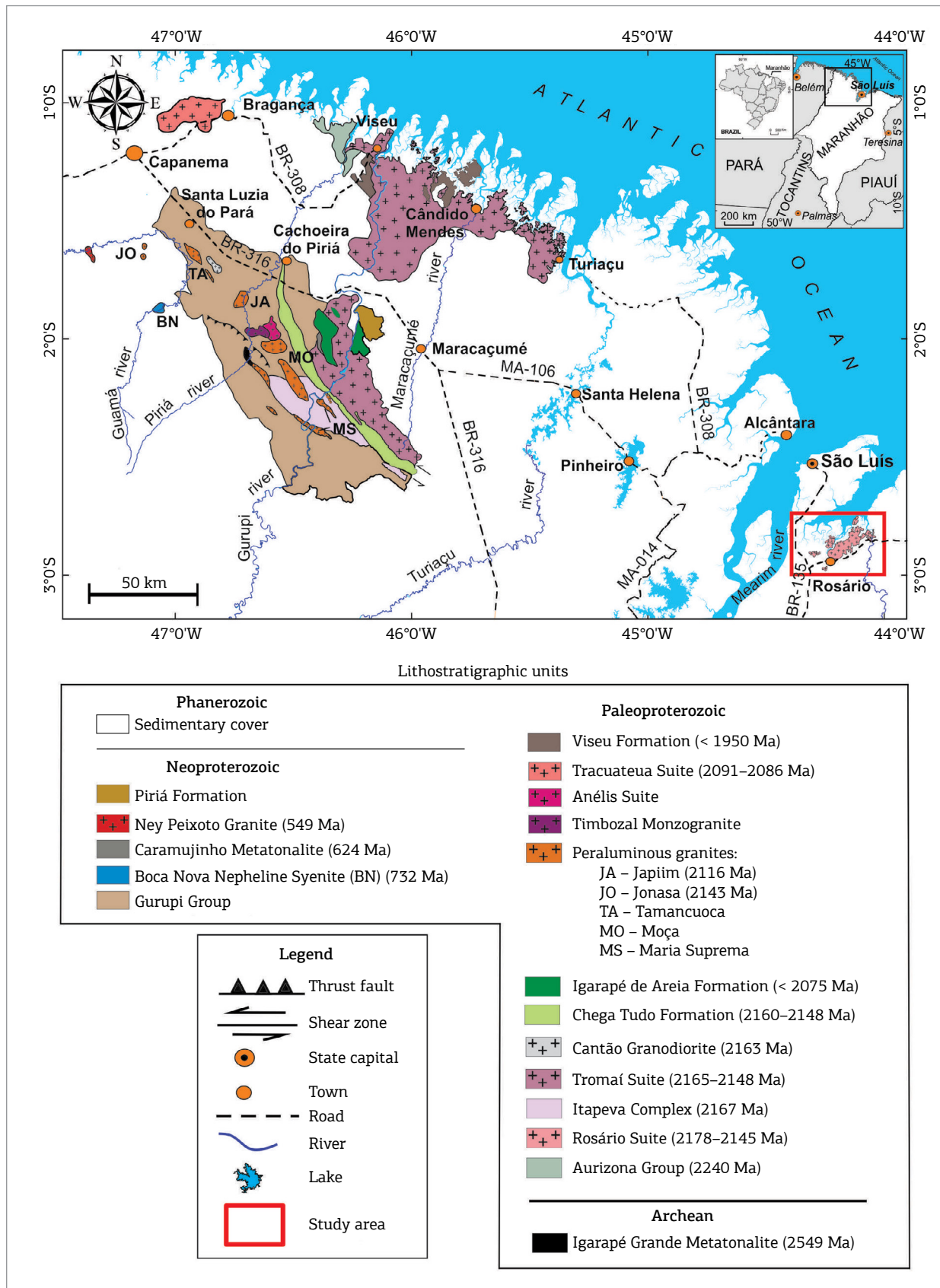


Figure 1. Simplified geological map of São Luis Craton and Gurupi Belt with the location of the study area in the northern state of Maranhão, northern Brazil. Adapted from Gorayeb et al. (1999), Vasquez and Rosa-Costa (2008), Klein et al. (2012) and Sousa et al. (2012). The cited geochronological ages are subject to variable analytical uncertainties.

genesis of reworked Archean to Paleoproterozoic crust, in clear contrast to the juvenile characteristics of the predominant magmatic unit of the neighboring Tromáí Suite (Klein *et al.* 2012).

## GEOLOGY OF THE ROSÁRIO REGION

The study area is located in the northwestern Maranhão State around the towns of Rosário, Bacabeira, Perizes, Axixá, Morros and Presidente Juscelino, where the Rosário Suite granitoids crop out (Fig. 2). The granitoids are exposed only in erosive and tectonic windows and are largely covered by Paleozoic sedimentary rocks of the Parnaíba Basin, in the southern portion, and the Cenozoic Barreiras Formation, in the north. The main exposures are found in mines and river valleys. Figure 2 shows the distribution of the principal units and the sampling locations.

In this work, we identified five main lithological types: meta-melatalonite, meta-tonalite, meta-granodiorite, meta-monzogranite, and andesite dykes. They are generally exposed in hill tops, gravel-extraction quarries and outcrop slabs on the banks and beds of rivers, such as the Rio Munim, in the town of Presidente Juscelino (Fig. 2) (in Appendix A are the coordinates of the points in the map).

The contact relationships between the rocks are not registered directly, but temporal relationships are recognized by the presence of enclaves or by injecting veins. The meta-tonalites contain many leucotonalite veins, pegmatites and aplites, which are genetically related to granodiorite nearby and the youngest magmatic phases of the suite, probably the most evolved felsic phases of magmatic differentiation of the suite (Gorayeb *et al.* 1999).

## ANALYTICAL PROCEDURES

### Petrography

Petrographic analyses of 16 thin sections from granitoids of the Rosário Suite were performed by conventional optical microscopy, involving mineralogical characterization and quantification and textural/microstructural analysis. Modal mineralogical analyses were performed using a Swift automatic point counter, with 2,800 points for each thin section (Table 1). Petrographic classification was defined according to Streckeisen (1976), Le Maitre (2002), Fettes and Desmons (2008) and Paschier and Trouw (1996), and the modal results were plotted in Q-A-P and Q (A + P) -M' diagrams.

### Geochemistry

The geochemical analyses were performed on 27 samples at the ACME Analytical Laboratories Ltd. (Vancouver, Canada)

and the analytical results are in Table 2. The analytical package included major and minor oxides and trace elements, including rare earth elements (REE).  $\text{SiO}_2$ ,  $\text{TiO}_2$ ,  $\text{Al}_2\text{O}_3$ ,  $\text{Fe}_2\text{O}_3$ ,  $\text{MgO}$ ,  $\text{CaO}$ ,  $\text{MnO}$ ,  $\text{Na}_2\text{O}$ ,  $\text{K}_2\text{O}$  and  $\text{P}_2\text{O}_5$  were analyzed by inductively-coupled plasma atomic emission spectrometry (ICP-AES), with detection limits of  $\text{SiO}_2 = 0.02\%$ ;  $\text{Al}_2\text{O}_3 = 0.03\%$ ;  $\text{Fe}_2\text{O}_3 = 0.04\%$ ; and  $\text{K}_2\text{O}$ ,  $\text{CaO}$ ,  $\text{MgO}$ ,  $\text{Na}_2\text{O}$ ,  $\text{MnO}$ ,  $\text{TiO}_2$ ,  $\text{P}_2\text{O}_5 = 0.01\%$ . Trace elements were analyzed by inductively-coupled plasma atomic mass spectrometry (ICP-MS) with detection limits of:  $\text{Ba}$ ,  $\text{Ga}$ ,  $\text{Hf}$ ,  $\text{Nb}$ ,  $\text{Rb}$ ,  $\text{Sr}$ ,  $\text{V}$ ,  $\text{Zr}$ ,  $\text{La}$ ,  $\text{Ce}$ ,  $\text{Eu}$ ,  $\text{Gd}$ ,  $\text{Dy}$ ,  $\text{Ho}$ ,  $\text{Er}$ ,  $\text{Tm}$ ,  $\text{Yb}$ ,  $\text{Co}$  and  $\text{Zn} = 0.5 \text{ ppm}$ ;  $\text{Cs}$ ,  $\text{Sn}$ ,  $\text{Cu}$  e  $\text{Ni} = 1 \text{ ppm}$ ;  $\text{Hg}$ ,  $\text{Ta}$ ,  $\text{Th}$ ,  $\text{Ti}$ ,  $\text{U}$ ,  $\text{W}$ ,  $\text{Y}$ ,  $\text{Sm}$ ,  $\text{Lu} = 0.1 \text{ ppm}$ ;  $\text{Bi}$ ,  $\text{Cd}$  e  $\text{Sb} = 0.1 \text{ ppm}$ ;  $\text{Pr}$  and  $\text{Pb} = 0.02 \text{ ppm}$ ;  $\text{Nd} = 0.4 \text{ ppm}$ .

Analytical accuracy was monitored by the analysis of the standard STD SO-18, chemical blanks and one duplicate analysis (sample 2013/SR-03). The detailed analytical procedures performed by ACME labs are available on <http://www.acmelab.com>. The concentrations of major elements were recalculated using the conversion factor for volatile correction, following the procedures of Rollinson (1993), Wilson (1989) and Gill (2010).

### U-Pb Geochronology

U-Pb zircon analyses were performed on five samples by laser inductively-coupled plasma mass spectrometry (LA-ICP-MS) at the Geochronology Laboratory of University of Brasília (UnB). The analytical procedures followed the recommendations of Bühn *et al.* (2009) and Chemale Jr. *et al.* (2012). The zircon crystals were concentrated using conventional techniques at the Pará-Iso Laboratory of the Federal University of Pará, in Belém, Brazil, including mineral sieving (250–180  $\mu\text{m}$  and 180–125  $\mu\text{m}$ ), magnetic separation and gravimetric separation by heavy liquid. The least magnetic zircon fraction was concentrated using an isodynamic Franz magnetic separator, and the least altered crystals were picked under a stereo microscope. Selected zircon grains were mounted in circular epoxy mounts and polished to obtain a smooth surface. Cathodoluminescence images were obtained using a scanning electron microscope (SEM) at the Geochronology Laboratory of UnB. U-Pb analyses were performed on a New Wave UP213 Nd:YAG laser ( $\lambda = 213 \text{ nm}$ ) coupled to a Thermo Finnigan Neptune Multicollector ICP-MS at frequency rate of 10 Hz, energy of approximately 100 mJ/cm<sup>2</sup>, and spot size varying from 15 to 30  $\mu\text{m}$ . The instrumental mass discriminations were corrected by the analyses of zircon standard GJ-1 (Jackson *et al.* 2004), and the instrumental mass discriminations were corrected by the standards GJ-1 zircon (Jackson *et al.* 2004) and 91500 zircon (Wiedenbeck *et al.* 1995).

Age calculations and U-Pb plots in the Concordia diagram were performed using Isoplot/Ex 3.0 software (Ludwig 2003). The estimate of common Pb was performed using

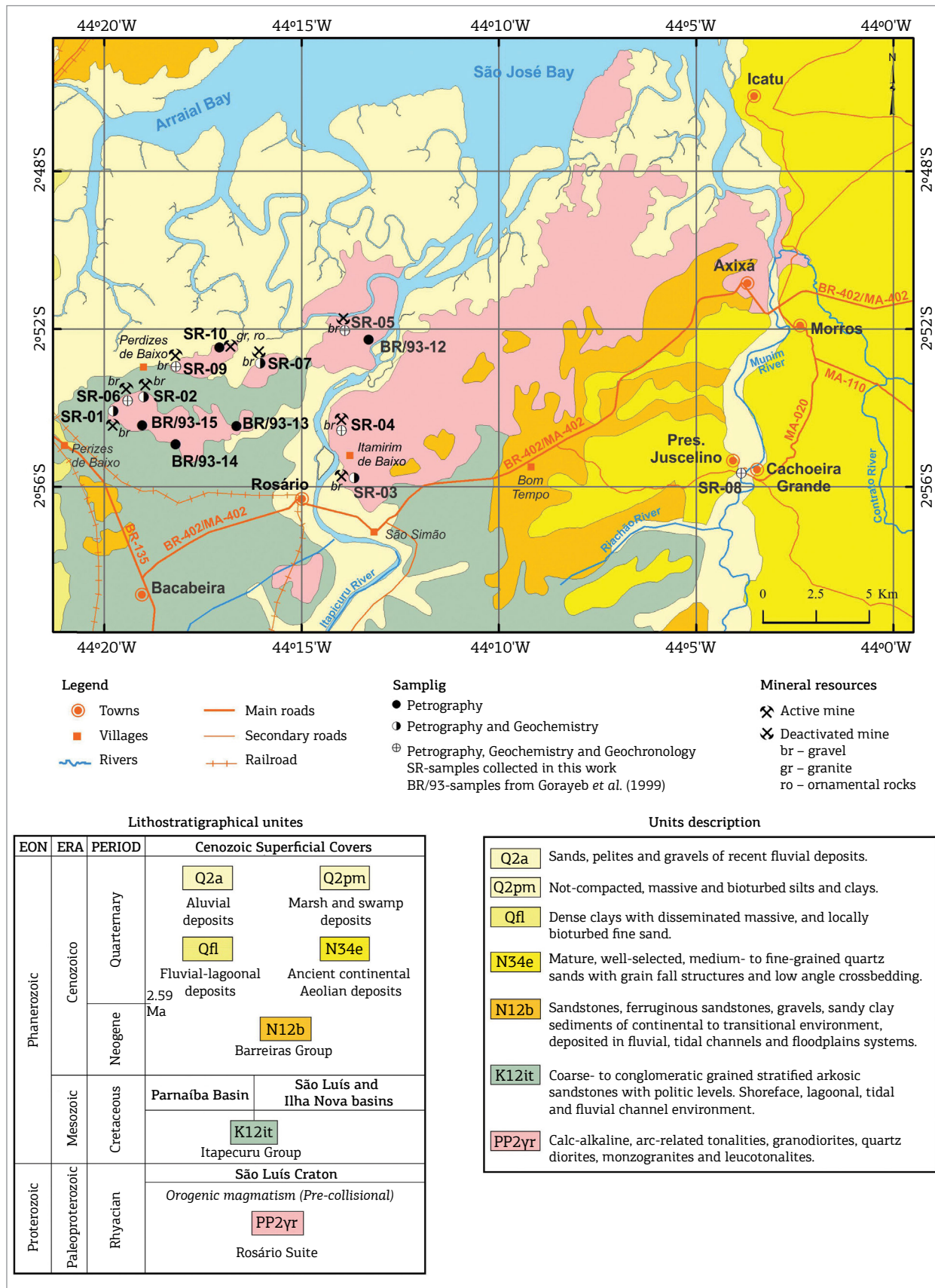


Figure 2. Geological map of the Rosário region with the localities of outcrops studied in this work. Modified from Gorayeb et al. (1999) and Sousa et al. (2012).

the model of Stacey and Kramers (1975), taking as reference the age  $^{206}\text{Pb}/^{208}\text{Pb}$  uncorrected for common Pb. The calculation and calibration procedures follow the routine of the Laboratory of Geochronology of the University of Brasília and are presented in Bühn *et al.* (2009). Only the uncertainties of the GJ-1 were propagated to the sample values; 91500 was treated as a secondary standard and analyzed as an unknown.

### Sm-Nd Isotopic Analyses

Sm-Nd isotopic analyses of four granitoids were performed at the Isotope Geology Laboratory (Pará-Iso Lab) of Geoscience Institute of Federal University of Pará following the analytical procedures of Gioia and Pimentel (2000) and Oliveira *et al.* (2008). Approximately 100 mg of whole-rock powders were mixed with 100 mg and  $^{149}\text{Sm}$ - $^{150}\text{Nd}$  spike solution and dissolved in Savillex capsules using the  $\text{HNO}_3$ , HF and HCl acids. Two-step ion-exchange chromatography was performed in Teflon columns, using the Ln Eichrom resin for Sm and Nd separation.

The Sm and Nd isotopic analysis was performed in a Thermo Finnigan Neptune Multicollector ICP-MS. For the correction of mass discrimination, the  $^{143}\text{Nd}/^{144}\text{Nd}$  ratio was normalized to  $^{146}\text{Nd}/^{144}\text{Nd} = 0.7219$ , using the exponential law (Russell *et al.* 1978). The accuracy and reproducibility of results

were controlled by standards using BCR-1 [ $(^{143}\text{Nd}/^{144}\text{Nd})$  ranged from  $0.512573 \pm 12$  ( $2\sigma$ ) to  $0.512669 \pm 10$  ( $2\sigma$ )], with the average value of  $0.512622 \pm 28$  ( $2\sigma$ ) and La Jolla ( $^{143}\text{Nd}/^{144}\text{Nd}$  isotopic ratios ranged from  $0.511793 \pm 9$  to  $0.511883 \pm 5$ , with most values being above 0.5118) (Oliveira *et al.* 2008). The decay constant used was  $6.54 \times 10^{-12} \text{ a}^{-1}$  (Lugmair & Marti 1978), and the Nd model ages (TDM) were calculated according to the model of depleted mantle evolution of DePaolo (1981). During the period of Sm and Nd procedures, total chemical blanks were lower than 0.1% of the elements concentration and were considered negligible.

### PETROGRAPHY OF THE ROSÁRIO SUITE

The plutonic rocks studied were classified according to Streckeisen (1976) and Le Maitre (2002) as quartz diorite, melatonalite, tonalite, granodiorite and monzogranite (Table 1, Fig. 3). Leucotalomite, pegmatite and aplite occur as veins, preferentially intruded into tonalitic rocks, which are also cross-cut by dykes of porphyry andesite. In general, the granitoids show variable deformation and low-grade metamorphism; primary igneous features are largely preserved (Fig. 4).

**Table 1. Modal composition of the Rosário Suite.**

Rock	Metaquartz diorite				Metamela-tonalites	Metatonalite							Metagranodiorite				
	1993/ BR-12a	1993/ BR-13	1993/ BR-14b	1993/ BR-15a		2013/ SR-05	2013/ SR-01	2013/ SR-02	2013/ SR-03	2013/ SR-04	2013/ SR-06	2013/ SR-09	1993/ SR-12b	2013/ SR-07	2013/ SR-08	2013/ SR-10	1993/ BR-14a
Sample	1993/ BR-12a	1993/ BR-13	1993/ BR-14b	1993/ BR-15a	2013/ SR-05	2013/ SR-01	2013/ SR-02	2013/ SR-03	2013/ SR-04	2013/ SR-06	2013/ SR-09	1993/ SR-12b	2013/ SR-07	2013/ SR-08	2013/ SR-10	1993/ BR-14a	
Pl	50.6	64.8	63.0	71.4	33.3	47.3	57.8	60.8	65.1	54.0	59.2	52.7	55.8	55.8	53.7	49.1	
Qtz	6.8	13.9	13.2	12.5	5.6	14.9	19.8	18.5	16.7	18.8	18.4	19.4	17.2	22.0	20.0	19.6	
Mic	1.9	5.4	6.1	6.8	0.2	3.8	0.4	0.6	1.0	6.7	3.4	6.7	9.9	8.1	8.8	16.8	
Hb	3.1	14.8	15.3	8.6	58.4	27.9	19.1	16.4	15.3	15.7	18.0	20.4	12.8	9.8	15.4	12.2	
Ttn	0.6	0.8	2.3	0.3	0.5	2.5	0.9	2.5	0.3	1.4	0.4	0.3	1.3	0.7	1.0	1.8	
Bt	0.4	0.2	-	-	1.1	1.4	0.3	0.5	-	1.1	0.2	-	1.1	2.3	0.3	0.2	
Opaque	-	-	-	0.3	0.1	0.4	0.1	0.2	0.6	0.3	-	-	0.1	0.3	0.3	0.1	
Apt	0.2	-	-	0.1	0.1	0.2	0.1	0.2	0.3	0.1	-	0.1	0.1	0.2	0.1	0.1	
Zrn	0.1	0.1	0.1	0.2	0.2	0.3	0.2	0.3	0.6	0.2	0.1	0.1	0.2	0.1	0.3	0.1	
Ep	0.3	-	-	-	0.1	0.7	0.6	-	0.1	1.2	0.3	0.3	1.1	0.7	0.1	-	
Total	100	100	100	100	100	100	100	100	100	100	100	100	100	100	100	100	
Felsic	59.9	84.2	82.4	90.8	39.9	67.8	79.6	80.4	83.8	81.5	81.4	79.3	84.7	86.9	86.9	83.0	
Mafic (M')	40.1	15.8	17.6	9.2	60.1	32.2	20.4	19.6	16.2	18.5	18.6	20.7	15.3	13.1	13.1	17.0	
100% recalculated	Q	6.84	13.91	13.21	12.34	5.65	15.17	20.12	18.59	16.87	19.18	18.47	19.50	17.52	22.22	20.92	19.12
	A+P	52.82	70.27	69.17	78.43	33.77	52.04	59.15	61.71	66.77	61.94	62.85	59.70	66.90	64.55	65.38	64.29
	M'	40.34	15.82	17.62	9.23	60.58	32.79	20.73	19.70	16.36	18.88	18.68	20.80	15.58	13.23	17.70	16.59
	Q	11.47	16.53	16.04	13.59	14.32	22.58	27.38	23.15	20.17	23.65	22.72	24.62	20.75	25.61	24.24	22.92
	A	3.20	6.42	7.41	7.52	0.51	5.76	0.52	0.75	1.21	8.43	4.20	8.50	11.94	9.43	10.66	19.65
	P	85.33	77.05	76.55	78.89	85.17	71.66	74.10	76.10	78.62	67.92	73.08	66.88	67.31	64.96	65.09	57.43

(2,800 points per sample with spacing of 2, values in %): Q: quartz; A: alkali-feldspar; P: plagioclase, M: mafic minerals.

Table 2. Chemical analyses of major, minor (in wt %) and trace elements (in ppm) for the Rosário Suite.

Rock	Metamelatonalite					Metaquartz Diorite					Metatonalite					Metagranodiorite						
	94-MA-05G	94-MA-SR-05	94-MA-01C1	94-MA-05E	94-MA-05D	94-MA-05B	94-MA-05PT	94-MA-02A	94-MA-SR-04	94-MA-SR-03	94-MA-SR-02	94-MA-SR-01	94-MA-SR-09	94-MA-SR-08	94-MA-SR-07	94-MA-SR-06	94-MA-SR-05	94-MA-SR-04	94-MA-SR-03	94-MA-SR-02		
SiO <sub>2</sub>	49.48	51.18	50.82	56.32	57.18	57.19	57.20	59.43	59.71	59.60	61.27	61.40	61.82	62.64	62.71	62.74	63.72	64.03	64.05	64.27	64.69	
TiO <sub>2</sub>	0.77	0.70	0.72	0.59	0.55	0.56	0.61	0.54	0.68	0.56	0.60	0.63	0.57	0.56	0.45	0.53	0.50	0.49	0.48	0.44	0.48	
Al <sub>2</sub> O <sub>3</sub>	14.49	16.32	15.23	15.25	15.96	15.31	15.43	15.19	16.47	15.89	15.11	16.17	15.52	15.49	16.79	15.27	15.23	15.37	15.31	15.39	16.22	
FeO.t	11.68	10.28	9.56	8.49	7.44	7.88	8.03	7.09	6.40	6.65	6.08	5.43	5.84	5.48	5.35	5.16	5.14	4.58	4.98	4.80	4.40	
MnO	0.22	0.18	0.18	0.16	0.15	0.15	0.15	0.15	0.12	0.13	0.09	0.12	0.09	0.09	0.10	0.08	0.08	0.08	0.07	0.09	0.02	
MgO	7.80	6.16	7.24	4.99	4.49	4.65	4.59	3.84	3.36	3.01	2.59	2.84	2.35	2.70	2.65	2.01	2.52	2.35	2.25	2.31	1.93	
CaO	8.81	8.77	7.28	5.11	6.98	6.38	6.62	6.11	2.98	6.29	5.00	4.09	5.25	4.41	4.44	5.30	3.96	3.39	4.27	4.22	3.70	
Na <sub>2</sub> O	2.37	3.09	2.63	1.82	3.66	2.49	2.61	3.21	2.81	4.30	4.10	3.60	3.53	4.05	3.93	4.58	3.96	4.38	4.00	4.50	4.23	
K <sub>2</sub> O	2.14	0.98	2.30	3.49	1.40	2.57	2.13	1.50	3.03	0.59	1.17	3.24	1.43	2.41	2.48	0.72	2.62	2.81	2.59	2.59	1.59	
P <sub>2</sub> O <sub>5</sub>	0.26	0.25	0.22	0.20	0.21	0.20	0.20	0.30	0.21	0.29	0.21	0.28	0.21	0.21	0.21	0.19	0.18	0.20	0.20	0.16	0.14	
LOI	2.5	1.9	3.4	3.1	1.7	2.3	2.1	2.6	3.5	1.5	2.6	3.1	2.5	1.6	1.7	1.7	2.1	1.4	1.2	1.8	1.9	
Total	100.52	99.81	99.58	99.52	99.70	99.68	99.84	99.66	99.10	99.78	99.71	99.70	99.68	99.61	99.76	99.69	99.64	99.69	99.72	99.70	99.77	
Ba	12234	407	1212	1939	566	1213	924	595	1387	303	723	1314	981	1346	1435	494	1190	1209	1204	1083	1168	926
Rb	47.2	20.5	45.6	83.5	34.8	60.5	46.9	58.9	67.4	25.3	69.0	50.6	46.6	48.0	49.0	46.9	51.9	51.9	54.6	53.5	55.5	19.9
Sr	1773.5	651.8	259.6	248.8	724.3	395.7	515.0	600.9	300.2	798.8	586.0	678.7	643.4	713.2	732.2	829.1	711.9	619.7	738.3	776.9	310.4	775.3
Zr	69.2	38.3	65.6	90.1	52.6	69.5	126.6	83.8	148.1	156.3	169.0	157.7	140.1	155.6	149.7	126.7	146.4	126.3	140.9	142.8	121.4	115.1
Nb	3.1	2.5	3.7	4.6	4.4	4.5	4.5	5.3	8.6	2.4	7.7	6.6	7.2	5.2	5.8	2.2	4.4	5.2	5.0	4.5	4.0	5.3
Y	18.1	15.9	19.2	18.4	14.9	16.1	16.5	16.4	14.9	15.3	19.9	13.0	18.0	16.0	14.2	9.6	12.0	14.0	14.1	12.2	11.2	12.7
Ga	15.2	15.9	16.7	15.3	16.3	15.4	15.2	15.4	16.7	17.5	16.9	16.4	17.2	15.8	15.8	16.3	14.5	14.7	17.1	17.6	16.9	12.1
Ni	19.5	15.5	21.6	15.9	20.5	17.8	15.6	13.4	6.8	9.7	6.9	13.3	13.4	6.4	7.9	7.7	8.0	8.6	7.2	9.3	4.5	5.2
Ta	0.3	0.2	0.2	0.4	1.2	1.0	0.2	1.1	1.5	0.2	0.5	0.6	1.0	0.2	0.1	0.2	0.4	0.6	0.3	0.5	0.3	1.6
Th	1.3	0.4	0.8	1.8	2.2	1.6	1.4	2.7	3.7	0.3	5.9	3.8	5.9	1.2	1.3	0.4	1.8	3.0	2.2	3.3	2.5	2.6
Cs	0.7	0.3	0.7	1.0	0.6	0.6	0.3	0.6	1.1	0.3	0.4	1.0	0.5	0.9	0.8	0.5	0.6	0.7	0.6	0.5	0.5	0.2
La	9.2	6.2	15.8	15.3	12.5	13.8	21.5	8.2	27.2	24.3	23.5	16.5	18.2	10.3	17.4	20.3	17.3	22.7	20.5	13.0	19.9	8.9
Ce	222.4	22.9	17.6	31.8	30.4	28.7	28.0	32.0	52.2	22.9	61.8	56.2	56.0	40.9	42.4	23.3	41.3	47.2	41.7	47.6	43.5	28.8
Pr	3.16	3.04	2.51	3.98	3.75	3.69	3.65	3.83	5.76	3.31	6.83	6.42	6.34	5.59	5.24	3.16	4.90	5.90	5.28	5.28	4.96	3.28
Nd	13.3	11.6	17.2	16.3	16.6	15.6	15.3	22.6	15.5	26.6	25.4	24.7	24.2	21.9	13.5	19.8	23.6	22.2	20.8	19.6	14.0	
Sm	3.28	2.91	3.26	3.67	3.18	3.35	3.33	3.50	5.17	4.85	4.84	4.10	2.78	3.42	4.31	4.22	3.86	3.54	2.58	2.69	3.05	1.80
Eu	0.95	1.01	1.04	1.05	1.01	1.02	0.95	0.94	1.23	1.07	1.47	1.10	1.37	1.15	1.05	0.91	0.92	1.01	1.00	0.96	0.89	0.77
Gd	3.18	3.01	3.44	3.32	2.88	2.95	3.03	3.07	3.53	3.15	4.45	3.55	4.29	3.66	3.28	3.23	3.07	3.31	3.08	3.03	2.94	2.42
Tb	0.35	0.51	0.59	0.55	0.48	0.48	0.50	0.49	0.57	0.51	0.75	0.52	0.68	0.56	0.47	0.36	0.45	0.51	0.48	0.47	0.39	0.42
Dy	3.01	2.81	3.63	3.16	2.46	2.70	2.67	2.71	3.14	3.08	4.20	3.69	2.96	2.35	2.11	2.32	2.78	2.35	2.48	2.02	2.52	1.07
Ho	0.64	0.66	0.66	0.53	0.57	0.58	0.54	0.58	0.77	0.50	0.67	0.53	0.50	0.42	0.42	0.49	0.50	0.46	0.39	0.54	0.18	
Er	1.89	1.77	2.10	1.87	1.54	1.54	1.70	1.57	2.11	1.52	1.84	1.48	1.35	1.10	1.23	1.57	1.39	1.25	1.12	1.50	0.51	0.14
Tm	0.29	0.25	0.30	0.29	0.24	0.24	0.27	0.25	0.22	0.27	0.32	0.27	0.25	0.21	0.18	0.18	0.21	0.18	0.16	0.25	0.08	0.02
$\Sigma$ ETR	65.78	63.84	55.28	83.59	77.74	76.13	74.54	79.72	118.97	65.83	144.03	128.55	130.35	104.19	102.53	61.62	96.86	112.81	101.29	101.07	110.44	13.40
Na <sub>2</sub> O+K <sub>2</sub> O	4.51	4.07	4.95	5.31	5.06	4.74	4.71	5.84	4.89	5.27	6.84	4.96	6.46	6.41	5.30	6.58	7.19	6.52	6.82	5.84	6.16	7.77
K <sub>2</sub> O/Na <sub>2</sub> O	0.90	0.32	0.87	1.92	0.38	1.03	0.82	0.47	1.08	0.14	0.29	0.90	0.41	0.60	0.63	0.16	0.66	0.64	0.63	0.61	0.37	0.26
La/N/YbN	11.38	12.25	6.81	3.07	3.50	9.24	5.77	25.31	13.08	9.71	2.05	8.95	8.52	12.22	9.23	9.72	9.37	6.23	8.70	4.91	10.87	5.47
Eu/Eu*	0.86	0.84	1.1	0.99	1.04	0.87	0.97	1.04	0.86	0.82	0.95	0.92	3.1	0.97	0.85	0.82	0.88	1.02	0.93	0.91	2.01	0.9
La/N/SmN	3.51	3.64	2.33	1.47	2.08	3.2	3.17	4.65	3.7	2.96	1.2	3.31	3.05	5.21	3.15	2.58	2.14	2.79	2.63	4.41	2.31	2.57
Gd/N/YbN	0.08	0.03	0.15	0.62	0.11	0.11	0.14	0.02	0.01	0.14	0.10	0.05	0.05	0.07	0.02	0.08	0.07	0.10	0.06	0.12	0.03	0.05

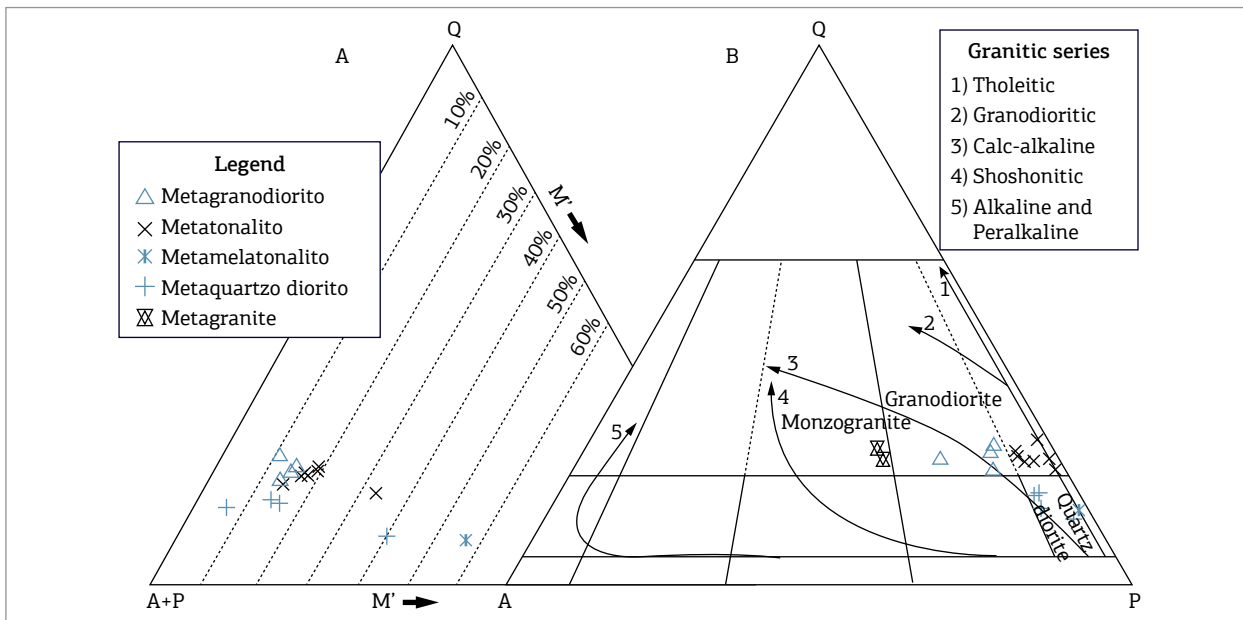


Figure 3. QAP and Q(A+P)M diagrams (Streckeisen 1976, Le Maitre 2002) with the modal composition of Rosário Suite rocks and displaying the composition trends of granitoid series from Lameyre and Bowden (1982).

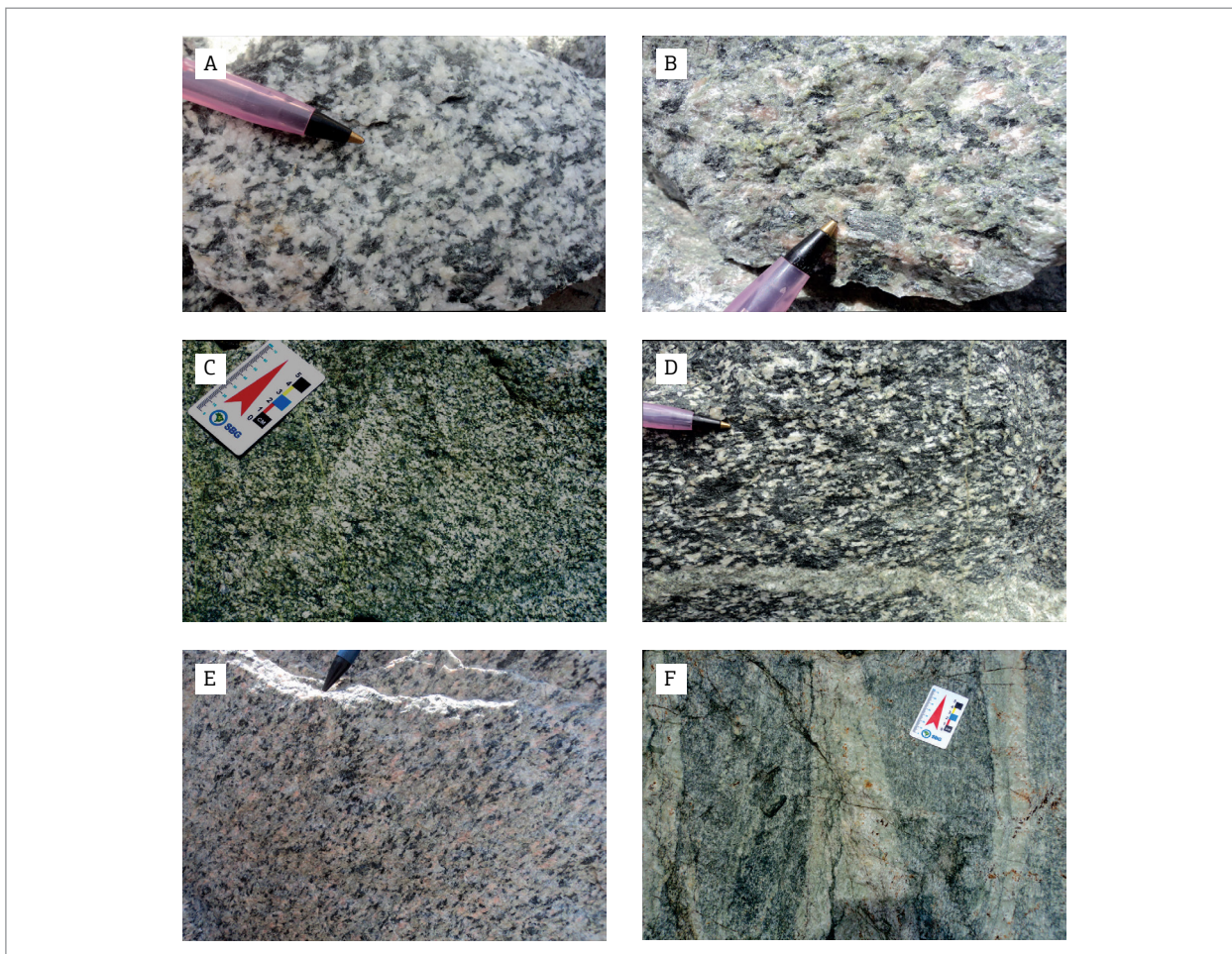


Figure 4. Textural and structural features of the Rosário Suite Granitoids: (A, B) relicts of igneous textures in granite and granodiorite; (C, D) metamelatalonites showing tectonic fabric; (E) preferred orientation of minerals in metagranodiorite; (F) metaleucotonalite with tectonic transposition banding and veins.

The granitoids are generally coarse-grained plutonic rocks with partially preserved hypidiomorphic granular texture. They are deformed by shearing in transcurrent zones, inducing partial mineralogical re-equilibration under greenschist metamorphic conditions that partially modified the plutonic igneous fabric, turning them into protomylonites. In this process, new mineral associations were generated (Chl, Ab, Act, Cc, Ep, Qtz), which changed the original grey and pink colors into green tones in these granitoids. Because of such characteristics, designation as metaplutonic rocks is more appropriate.

### Hornblende metatonalite

The hornblende metatonalites are phaneritic coarse-grained, and leucocratic to mesocratic ( $M = 16-32$ ), with greenish and whitish light grey colors. Medium-to fine-grained portions are related to comminution in shear zones and show discrete foliation defined by the preferred orientation of feldspars, quartz, biotite and amphibole. The preserved textural aspects in these rocks have two main characteristics: plutonic igneous textures (e.g., hypidiomorphic granular type) and the superposition of a tectono-metamorphic fabric recognized by overlapping mineral grains resulting in rock anisotropy, which becomes mylonitic foliation in shear zones or shear bands. This anisotropy is a common feature in the Rosário Suite rocks. The essential primary mineralogy comprises oligoclase ( $An_{24}$ ), quartz, hornblende and biotite. Accessory minerals are titanite, apatite, zircon and opaque minerals. Secondary phases, related to metamorphic transformations, are represented by tremolite-actinolite that partially replaces hornblende, and plagioclase transformed into epidote and sericite by saussuritization.

### Hornblende-biotite metatonalite

Of restricted occurrence (2013/SR-05), it represents a variation of the hornblende metatonalite. This sample exhibits coarse grain-size and a melanocratic colour index ( $M = 60-70$ ): dark grey, with greenish and whitish tones. Microscopically, it shows hypidiomorphic granular texture and mineralogy represented by oligoclase ( $An_{25}$ ), quartz, microcline, hornblende, biotite and titanite, with accessory apatite, zircon and opaque minerals. Tremolite-actinolite, epidote and sericite represent secondary phases related to metamorphic transformation.

### Hornblende metagranodiorite and Hornblende metaquartz diorite

The hornblende metagranodiorite and hornblende metaquartz diorite are leuco- to mesocratic ( $M = 9-40$ ), coarse-grained and pinkish grey rocks, showing hypidiomorphic

granular texture. Plagioclase, quartz, microcline, hornblende and titanite are the main mineralogical phases, with biotite, apatite, zircon and opaque minerals as accessories. The alteration phases are tremolite-actinolite, sericite and epidote. The textural aspects are similar to those of metatonalite, e.g., preserved plutonic features in a mylonitic fabric. The feldspars, amphibole and quartz crystals are rotated and slightly stretched, forming an incipient foliation. In these rocks, centimetre-thick dioritic or amphibole-rich mafic enclaves are also found, representing fractions of partially digested tonalite (Fig. 5A).

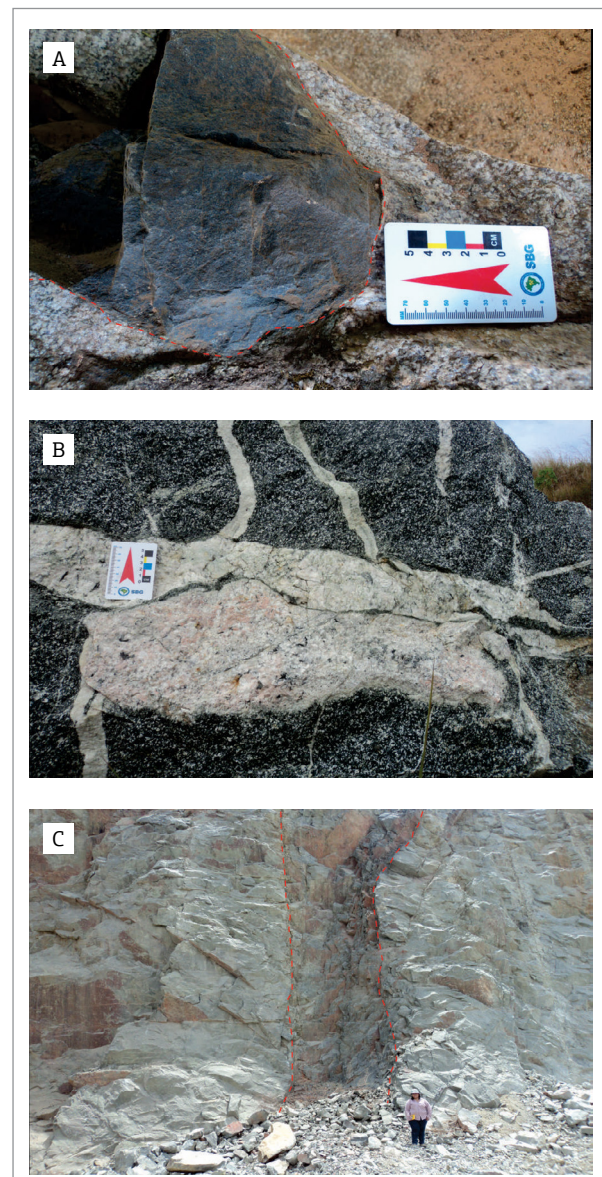


Figure 5. General features of the Rosário Suite Granitoids: (A) mafic enclave enclosed by granodiorite; (B) network of leucogranite veins cutting melatonalite; (C) subvertical dykes of porphyritic andesite cutting granitoids in the quarry walls.

## Metamonzogranite

Monzogranitic rocks are coarse-grained, slightly richer in quartz and alkali-feldspar, plagioclase and biotite, and lacking hornblende. The textures are similar to the types described before with minerals slightly imbricated due to deformation and incipient recrystallization. The plagioclase crystals exhibit green tones due to saussuritization, and epidote, sericite and calcite transformation.

The field and petrographic data of granites series studied reveals an important plutonic event in the region in which all rocks show petrographic similarities with common textural and mineralogical features, reflecting slight variations in mineral quantities. As shown in Figure 4, the compositional trends suggest magmatic differentiation processes in the evolution of this suite, as pointed out by Gorayeb *et al.* (1999).

## STRUCTURAL GEOLOGY AND THERMAL-TECTONIC PROCESSES

The granitoids of Rosário Suite exhibit textural/structural and mineralogical changes related to shear tectonics recorded in other parts of the São Luís Craton, as well as faults and joints. However, except along the shear zones, these transformations did not destroy the original igneous fabric, which preserves the history of plutonic origin. The main structural features superimposed on igneous textures are marked by imbrications and light stretching of the primary minerals (quartz, plagioclase, hornblende and titanite), creating anisotropy and developing a discrete foliation in the rocks, transforming them into protomylonites.

Shear bands and ductile shear zones with sinistral movement, centimetric to decimetric widths and lengths up to tens of meters, are common in the study area. Along these zones, there is a 50–70° Az mylonitic foliation that dips between 60 and 70° SE and stretching lineation dipping 30–35 to 200–220 Az. In some narrow zones, mylonite and ultramylonite developed, marked by darker colour and comminution of minerals, resulting in aphanitic rocks. The microstructural features are highlighted by almond-shaped hornblende and relict plagioclase, and quartz ribbons in a fine-grained matrix. The matrix is composed of sericite, epidote and carbonates replacing plagioclase, associated with quartz and plagioclase microgranular aggregates, chlorite, acicular tremolite-actinolite and microgranular titanite derived mainly from the substitution reaction of hornblende.

In general, the granitoids are slightly deformed with incipient metamorphic transformation that generated new

mineral assemblages, imposing green tonalities on the original grey and pink colours and these granitoids. The metamorphic paragenesis Ab + Ser + Ep + Chl + Act + Cc + Qtz coexists with relict primary minerals (quartz, plagioclase, hornblende, alkali-feldspar), which allows us to estimate the metamorphic conditions in the low greenschist facies.

The transformations recorded in Rosário Suite may be related to the same context of thermo-tectonic processes that took place on other areas, such as to the boundary between the craton and the Gurupi Belt (Klein & Lopes 2011).

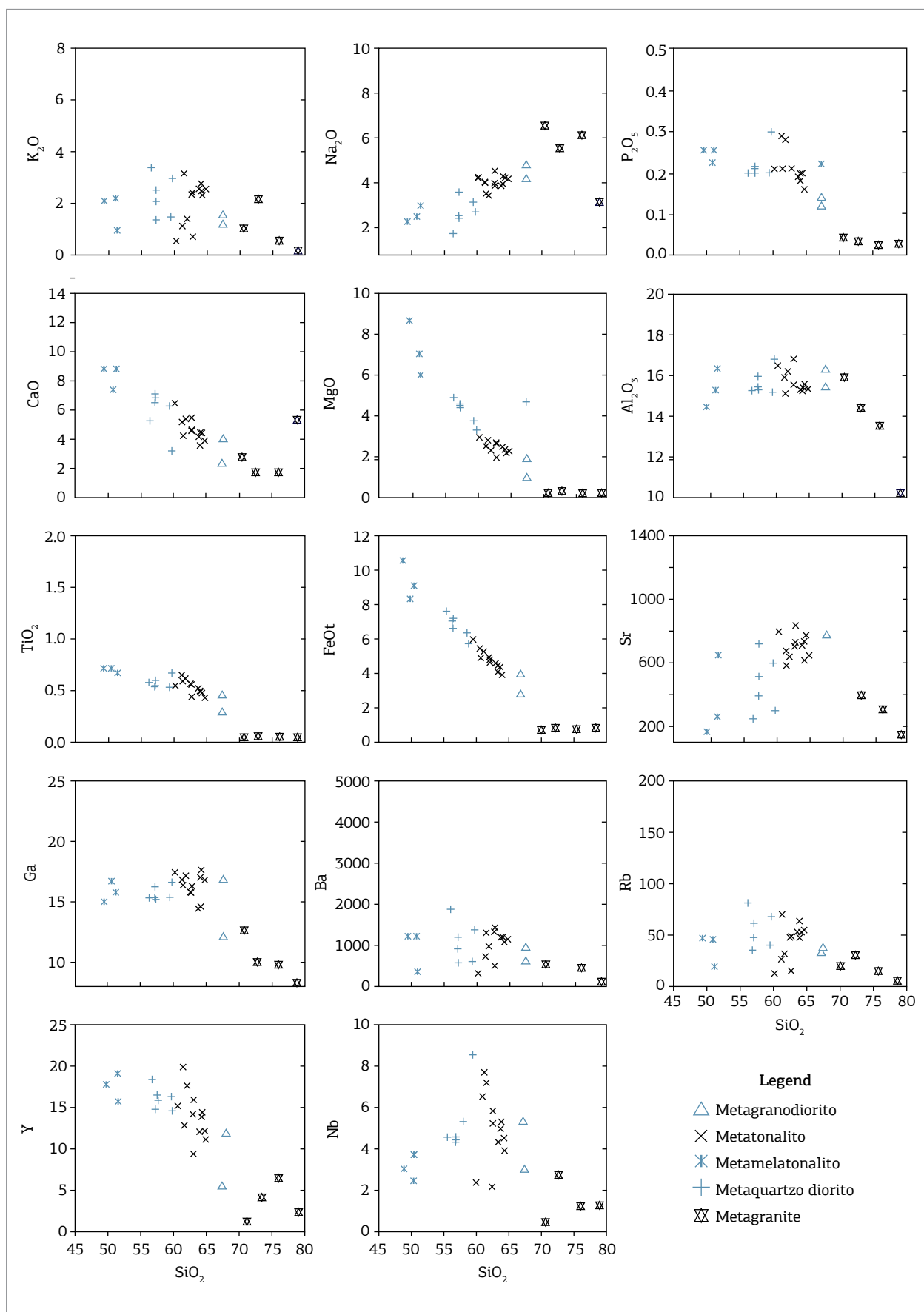
## GEOCHEMISTRY OF THE ROSÁRIO SUITE

In general, the studied granitoids demonstrated high contents of SiO<sub>2</sub> (50–79%), Al<sub>2</sub>O<sub>3</sub> (10–16%) and Na<sub>2</sub>O (2.3–6.7%) and low concentrations of TiO<sub>2</sub> (0.03–0.77%), K<sub>2</sub>O (0.6–3.5%), MnO (0.02–0.22%) and P<sub>2</sub>O<sub>5</sub> (0.02–0.3%). Other major elements showed low and moderate variations: MgO (0.12–8%); CaO (1.5–9%); Fe<sub>2</sub>O<sub>3</sub><sup>Total</sup> (0.8–12%); Na<sub>2</sub>O (1.8–7%); and low K<sub>2</sub>O/Na<sub>2</sub>O ratio (0.1–1.9). The trends of compositional types (diorite, tonalite, granodiorite and granite) showed continuous variation in the contents of main major and trace elements, with increasing SiO<sub>2</sub>, with positive covariance between Na<sub>2</sub>O and SiO<sub>2</sub>, and negative covariance between CaO, Fe<sub>2</sub>O<sub>3</sub><sup>t</sup>, K<sub>2</sub>O, MgO, TiO<sub>2</sub> and P<sub>2</sub>O<sub>5</sub> (Fig. 6). These variations are probably related to magmatic differentiation.

In classificatory diagrams, as R<sub>1</sub>-R<sub>2</sub> (La Roche 1980) and diagram Total-Alcali vs. Silica (TAS) (Cox *et al.* 1979), all granitoids plot in the fields of diorite, tonalite, granodiorite and granite (Fig. 7A, B), in accordance with the petrographic classification. The samples that fall in the gabbro field are melanocratic types (melatonalites and diorites).

In the aluminum-saturation Shand diagram (Shand 1950) (Fig. 8), the granitoids plot within the metaluminous field, followed the petrographic data that show significant presence of hornblende and minor biotite. In the diagram Alkali oxides, Fe oxides e Magnesium (Mg), the rocks define a trend compatible with the calc-alkaline series (Fig. 9).

In the multielement diagram, the compositional groups showed consistent signatures (Fig. 10), such as large-ion lithophile elements (LILE)-enrichment relative to light rare earth elements (LREE) and high field strength (HFS) elements. Furthermore, the geochemical pattern of quartz diorites and granodiorites are similar, showing positive Ba and negative Th anomalies.

Figure 6. Harker diagrams with major and trace elements vs.  $\text{SiO}_2$  for granitoids of the Rosário Suite.

Metatonalites are similar to tonalites, exhibiting accentuated negative Th and Nb anomalies with fractionated patterns. Granites also demonstrate more accentuated sub-horizontal pattern with the most intense high field strength elements (HFSE) depletion.

The rare earth elements (REE) patterns are very similar for all analyzed granitoids. However, three groups can be discriminated. The first one, composed of quartz diorite and tonalite, shows sub-horizontal heavy rare earth elements (HREE) pattern and steep LREE pattern, which is slightly fractionated, with La/Yb ratio between 2 and 13, and

incipient negative Eu anomalies. The second group, consisting of granodiorites and granites, exhibits steeper REE patterns than the other two groups ( $\text{La/Yb} = 3\text{--}22$ ), with slight heavy REE depression and incipient negative Eu anomalies [ $(\text{Eu}/\text{Eu}^*)_{\text{N}} = 0.9\text{--}2.0$ ]. In general, the total REE content is lower ( $\sum_{\text{REE}} = 13$  to 89 ppm) than in the quartz diorite and tonalite ( $\sum_{\text{ETR}} = 55$  to 144 ppm) (Fig. 11).

In the  $\text{Y} + \text{Nb}$  versus  $\text{Rb}$  (Pearce *et al.* 1984) and  $\text{Zr}$  versus  $(\text{Nb}_{\text{N}}/\text{Zr}_{\text{N}})$  (Thiéblemont & Tégyey 1994) diagrams the rocks plot in the field of volcanic arc granites (VAG) related to subduction setting and calc-alkaline affinity

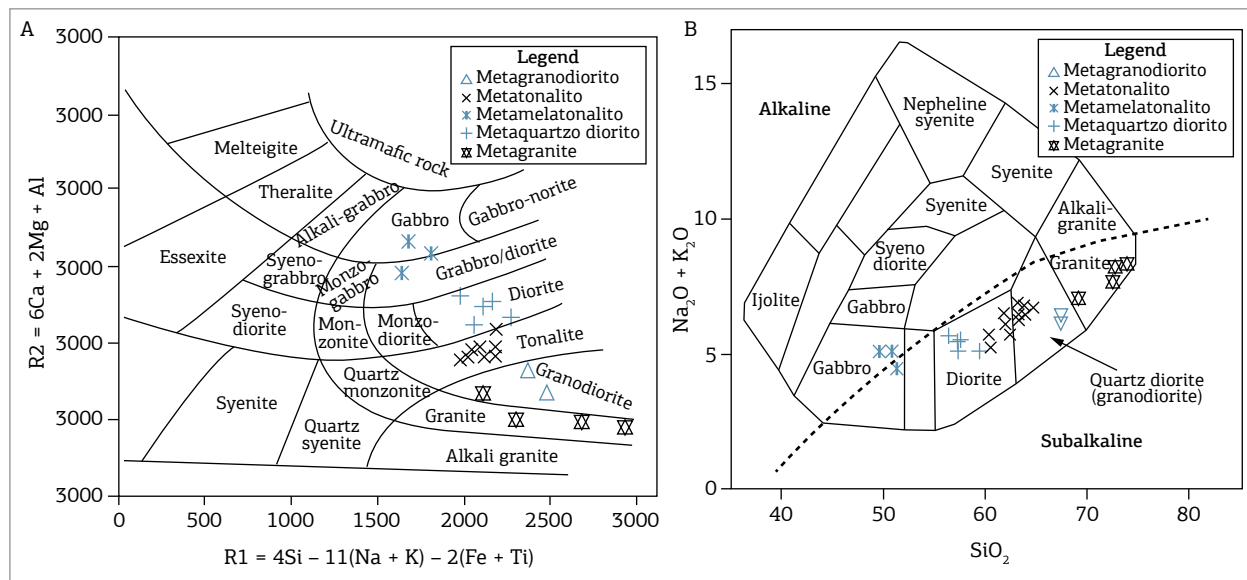


Figure 7. Geochemical diagrams with plotted data of the Rosário Suite Granitoids: (A)  $\text{R}_1$ - $\text{R}_2$  classification diagram (La Roche 1980); (B) TAS classification diagram (Cox *et al.* 1979).

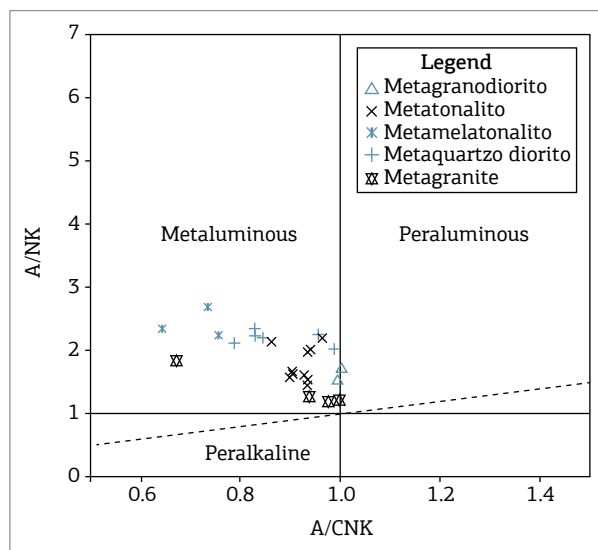


Figure 8. Rosário Suite plotted in the aluminum saturation diagram (Shand 1950).

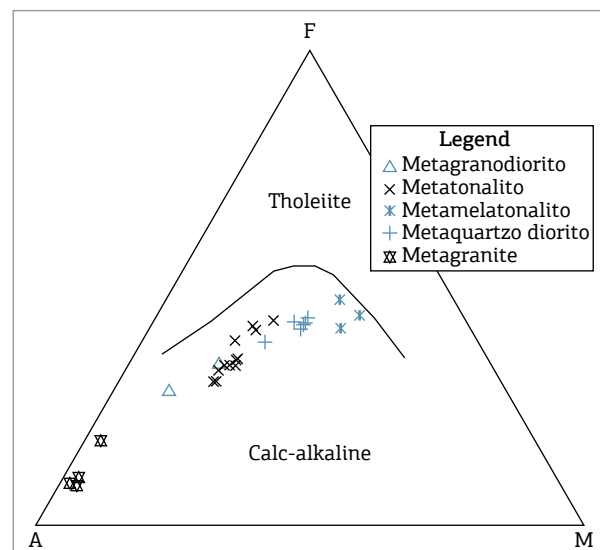


Figure 9. AFM diagram for magmatic series classification (Irvine & Baragar 1971) with the Rosário Suite trends.

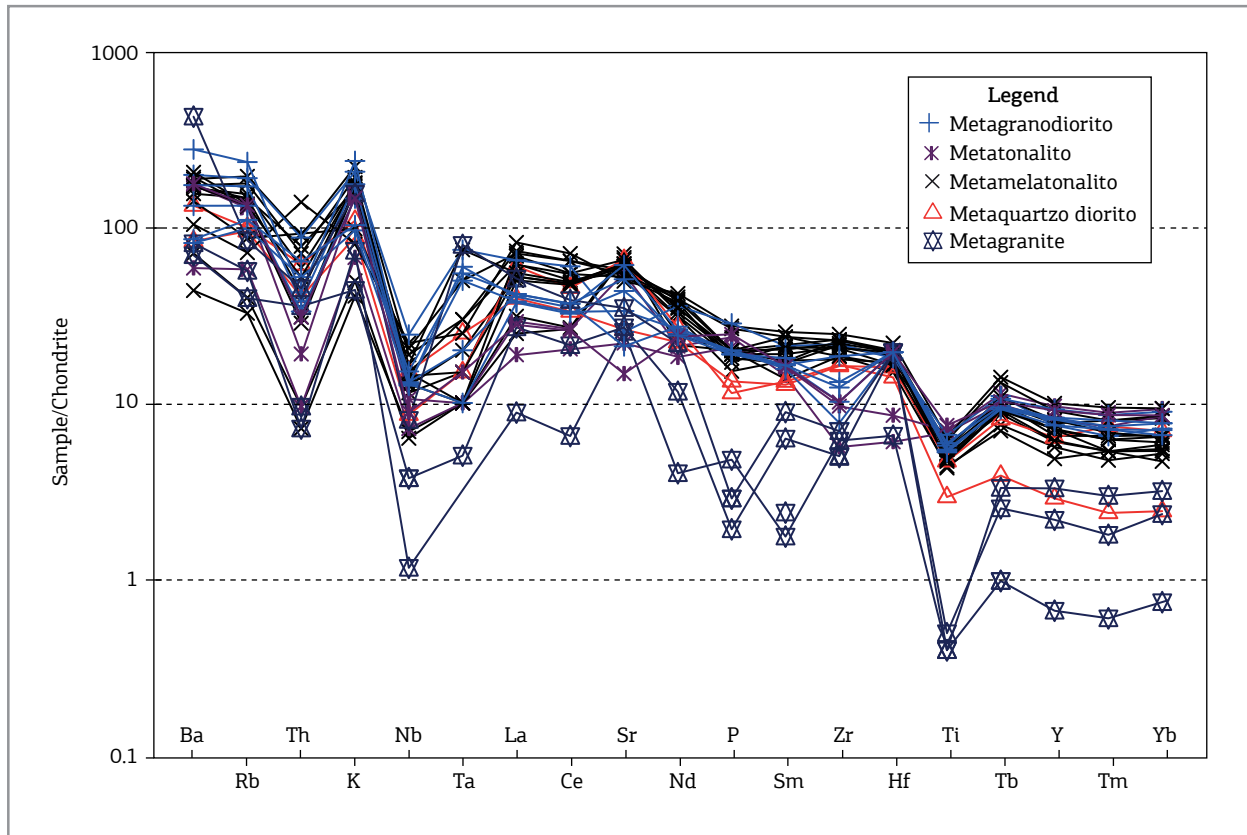


Figure 10. Chondrite-normalized multielement diagram (Thompson 1982) for the granitoids of the Rosário Suite.

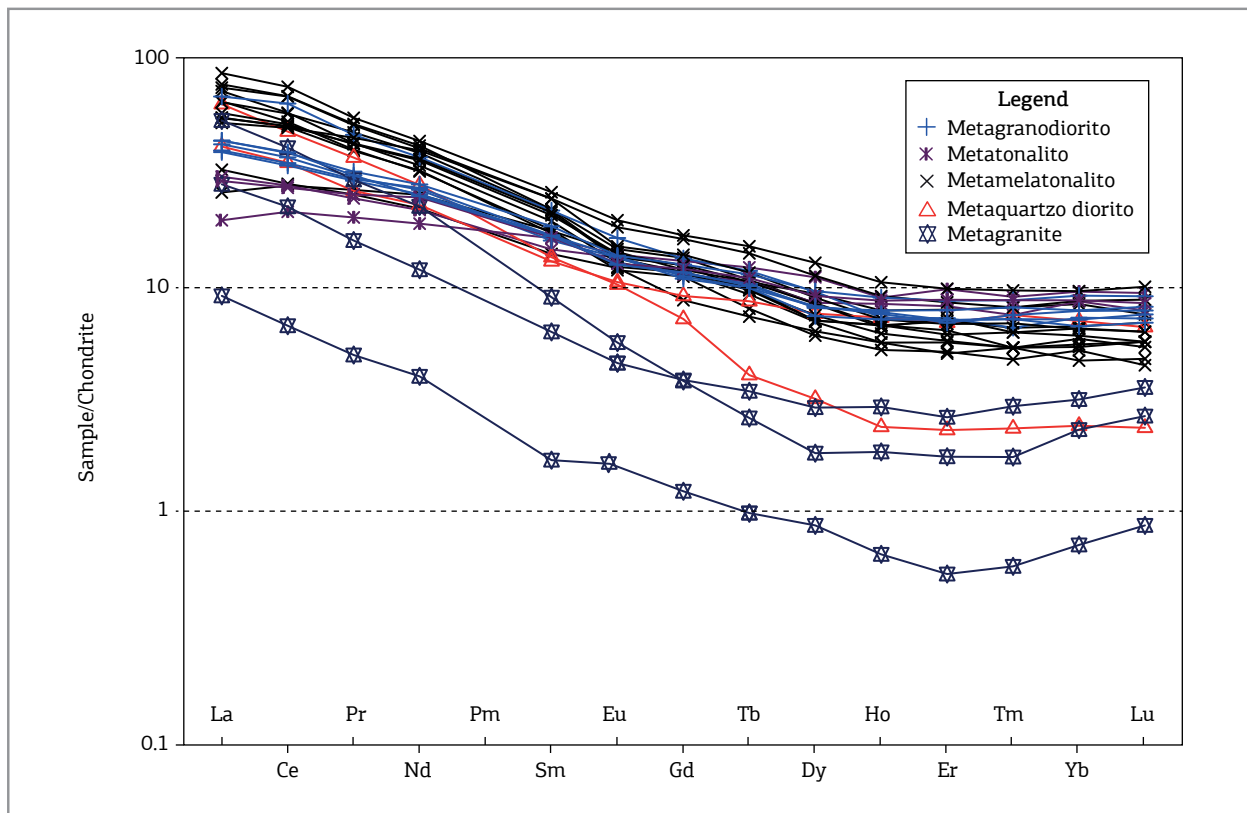


Figure 11. Rare earth element (REE) diagrams normalized to chondrite (Boynton 1984) for the Rosário Suite rocks.

(Fig. 12A, 12B). In the log  $[\text{CaO}/(\text{Na}_2\text{O}+\text{K}_2\text{O})]$  versus  $\text{SiO}_2$  diagram (Brown *et al.* 1984), the studied rocks correspond to granites of normal continental arc, similar to the Sierra Nevada and Peru batholiths of North and South America, respectively (Winter 2001, Mc Birney & White 1982, Thorpe *et al.* 1982) (Fig. 12C).

## U-PB GEOCHRONOLOGY

Petrographic analyses under optical microscope and stereomicroscope observations of zircon grains complemented by cathodoluminescence (CL) images identified mostly

euhedral zircon crystals with well-defined faces, showing clear concentric magmatic zoning (Fig. 13). The least magnetic zircon grains were chosen for analysis, and the analytical points were chosen considering the more homogeneous portions of the crystal, without inclusions or fractures. Analyses of the nucleus and edge of the crystals presented similar results. The results of the geochronological analyses are in Tables 3 to 7. Most of the analyzed zircon grains have Th/U ratios between 0.23 and 0.90, within the normal range for magmatic zircons.

The age uncertainties calculated are all 2-sigma, or 95% confidence, limit uncertainties based on internal reproducibility of the sample data, but they do not take into account

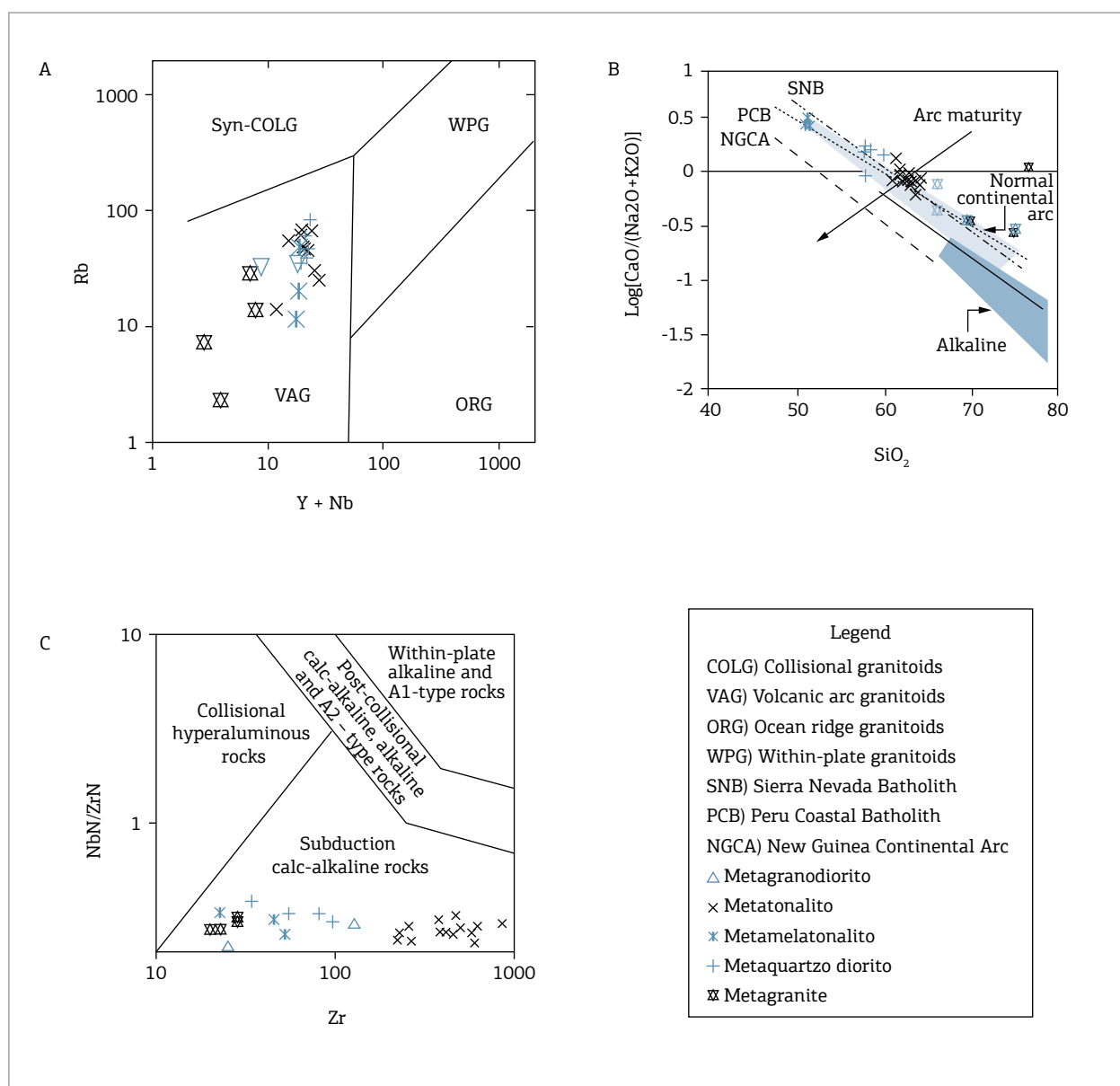
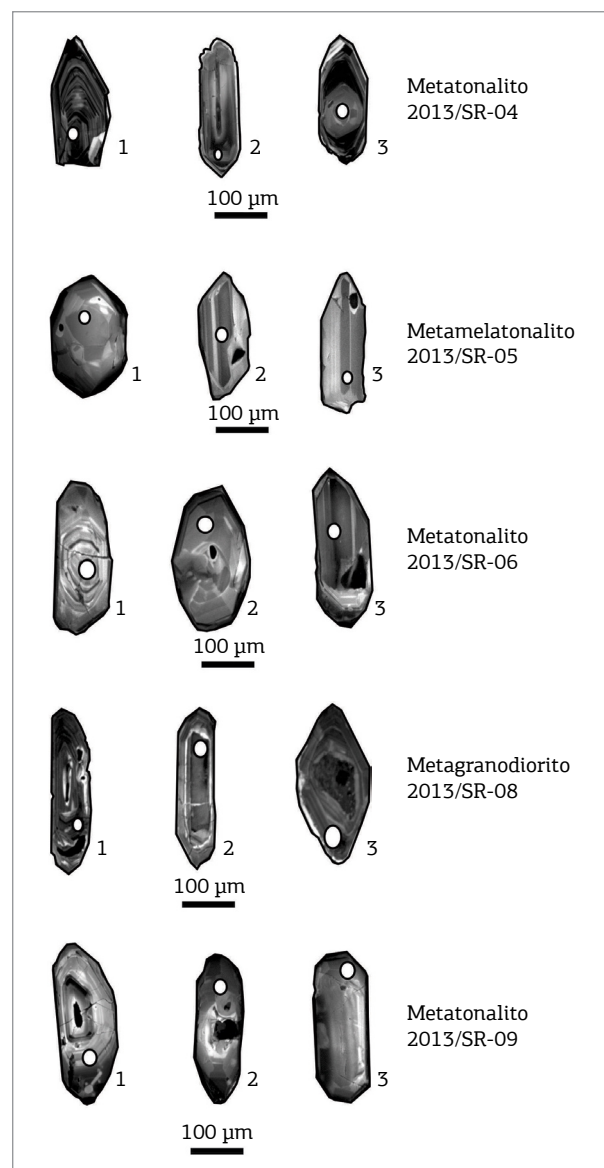


Figure 12. Geochemical diagrams for tectonic environment classification: (A)  $\text{Y}+\text{Nb}$  versus  $\text{Rb}$  (Pearce *et al.* 1984); (B)  $\log [\text{CaO}/(\text{Na}_2\text{O}+\text{K}_2\text{O})]$  versus  $\text{SiO}_2$  (Brown *et al.* 1984); (C)  $\text{Zr}$  versus  $\text{Nb}_{\text{N}}/\text{Zr}_{\text{N}}$  (Thiéblemont & Tégyey 1994).

the equivalent uncertainty in U/Pb calibration against the standards, normally no better than around 0.3%.

The total of 29 zircons were analyzed from sample 2013/SR-04 (metatonalite), which fall around a line with an upper intercept at  $2170 \pm 4$  Ma (Mean Square of Weighted Deviated — MSWD = 1.0, Fig. 14A). A more robust age estimate for the original crystallization is a Concordia age (as evaluated by Ludwig 2003) of  $2166 \pm 7$  Ma (MSWD = 0.02) for the seven most concordant data points.

Twenty-nine analyses from a second metatonalite sample (2013/SR-05) gave a slightly more concordant dataset



**Figure 13.** Cathodoluminescence images of analyzed zircon grains from the Rosário Suite Granitoids. Open circles mark spots analyzed by LA-ICP mass spectrometer (15–30  $\mu\text{m}$ -size).

(Fig. 14B) with an upper intercept age of  $2170 \pm 6$  Ma (MSWD = 0.7) and a poorly constrained lower intercept of  $-158 \pm 370$  Ma. In this case, nine of the data points provided a Concordia age of  $2170 \pm 7$  Ma (MSWD = 1.3).

Twenty-five zircons were analyzed from metatonalite sample 2013/SR-06; all are somewhat discordant (Fig. 14C), and the best age that can be obtained is the weighted mean  $^{207}\text{Pb}/^{206}\text{Pb}$  age of  $2170 \pm 7$  Ma (MSWD = 1.7) (Fig. 14D).

The single metagranodiorite sample analyzed (2013/SR-08) yielded 23 data points with a wide spread in the Wetherill diagram (Fig. 14E), but with variable non-linear discordance. The best estimate for the original crystallization age is taken as the weighted mean  $^{207}\text{Pb}/^{206}\text{Pb}$  age of  $2176 \pm 8$  Ma for the nine most concordant data (MSWD = 0.5) (Fig. 14F).

For the final metatonalite sample (2013/SR-09), a set of 29 zircons was analyzed (Table 6, Fig. 14G). The data are variably discordant and do not fit a straight line in the Wetherill diagram. Too few are sufficiently concordant to define a Concordia age, but 21 analyses that are less than 5% discordant, given a weighted mean  $^{207}\text{Pb}/^{206}\text{Pb}$  age of  $2,161 \pm 4$  Ma (MSWD = 0.7).  $^{207}\text{Pb}/^{206}\text{Pb}$  ages are equivalent to forcing a Discordia though zero, which in this case gives a close minimum age for crystallization (Fig. 14H).

The graphical representation of T (Ga) *versus*  $\epsilon\text{Nd}$  (Fig. 15) also shows that all the new results fall within the field corresponding to juvenile Paleoproterozoic crust of the São Luís Craton, compiled from the data of Klein *et al.* (2005a, 2012).

These results and the geochemical data reveal the juvenile nature of these rocks reinforcing the interpretation that this region may be part of the Rhyacian juvenile continental magmatic arc, that extends through other parts of São Luís Craton with correspondence in the northeast portion of the Amazonian Craton and in West Africa (Abouchami *et al.* 1990, Boher *et al.* 1992, Wright *et al.* 1995, Hirdes *et al.* 1996).

## WHOLE-ROCK Sm-Nd RESULTS

The Sm and Nd isotopic analytical results of four samples of metatonalites from the Rosário Suite (Table 8) showed acceptable value ranges for both  $^{147}\text{Sm}/^{144}\text{Nd}$  ratio (0.08 to 0.13) and fractionation degree (-0.54 to -0.39), according to Sato and Tassinari (1997).

The  $\epsilon\text{Nd}$  values calculated according to the crystallization age obtained in this work ( $t = 2.2$  Ga) are in the range +3.2 to +1.9 and the data yield similar  $T_{DM}$  model ages for separation from depleted mantle of 2.21 to 2.31 Ga.

Table 3. Summary of U-Pb zircon in situ data from sample obtained by LA-MC-ICP-MS from metatonalite (SR-04) of the Rosário Suite.

Zircon spot	$f_{\text{206}}$ (%)	U (ppm)	Pb (ppm)	Th (ppm)	Th/U	$^{207}\text{Pb}/^{235}\text{U}$	1s (%)	Rho	Ratios #			Ages (Ma)		
									$^{206}\text{Pb}/^{238}\text{U}$ (%)	$^{207}\text{Pb}/^{206}\text{Pb}$ (%)	1s $^{206}\text{Pb}/^{238}\text{U}$ (abs)	$^{207}\text{Pb}/^{235}\text{U}$ (abs)	1s $^{207}\text{Pb}/^{206}\text{Pb}$ (abs)	
Z1	0.01	51	23	18	0.36	7.091	1.0	0.378	1.0	0.95	0.136	0.3	2069	17
Z2	0.01	38	17	19	0.50	7.222	1.2	0.386	1.1	0.87	0.136	0.6	2104	19
Z10	0.01	69	33	41	0.59	7.026	0.8	0.377	0.7	0.83	0.135	0.4	2061	12
Z13	0.01	79	38	29	0.37	7.304	0.9	0.392	0.7	0.84	0.135	0.4	2130	13
Z16	0.01	96	46	38	0.40	6.816	0.8	0.365	0.7	0.90	0.135	0.3	2006	15
Z20	0.01	90	32	21	0.23	7.168	0.8	0.383	0.7	0.81	0.136	0.4	2090	12
Z3	0.01	45	21	16	0.35	7.298	0.8	0.388	0.7	0.83	0.136	0.4	2114	12
Z4	0.02	21	10	5	0.25	7.500	1.5	0.395	1.0	0.76	0.154	0.8	2147	19
Z5	0.01	25	11	9	0.37	6.997	1.1	0.375	0.8	0.72	0.135	0.8	2055	15
Z6	0.05	85	37	57	0.68	5.501	1.3	0.298	1.1	0.85	0.134	0.7	1681	17
Z7 **	0.01	82	39	27	0.33	7.490	0.7	0.401	0.6	0.87	0.135	0.3	2173	11
Z8 *	0.01	37	16	8	0.23	8.445	2.0	0.457	1.7	0.83	0.134	1.1	2427	33
Z9	0.01	67	30	23	0.34	6.967	0.7	0.375	0.6	0.85	0.135	0.4	2051	11
Z11	0.00	76	38	26	0.34	7.746	1.0	0.413	0.9	0.93	0.136	0.4	2227	18
Z12	0.01	112	51	49	0.44	6.757	0.7	0.365	0.6	0.84	0.134	0.4	2005	11
Z14	0.01	54	26	23	0.44	7.189	0.8	0.387	0.7	0.81	0.135	0.4	2107	12
Z17	0.01	90	43	35	0.39	6.983	1.0	0.372	0.9	0.91	0.136	0.4	2041	15
Z18 **	0.01	73	36	22	0.30	7.490	1.0	0.403	0.9	0.93	0.135	0.3	2182	17
Z19	0.01	37	17	11	0.31	7.071	0.9	0.382	0.7	0.84	0.134	0.4	2087	13
Z21	0.01	101	46	44	0.44	7.159	0.7	0.384	0.6	0.87	0.135	0.3	2096	11
Z22 **	0.01	38	18	14	0.38	7.456	0.9	0.400	0.8	0.83	0.135	0.5	2170	15
Z23	0.01	75	37	33	0.45	7.685	0.9	0.412	0.9	0.92	0.135	0.4	2223	16
Z24 **	0.01	80	39	30	0.38	7.497	0.8	0.402	0.8	0.88	0.135	0.4	2179	14
Z25 **	0.01	43	20	16	0.38	7.468	1.1	0.401	1.0	0.91	0.135	0.4	2172	18
Z26	0.00	157	77	113	0.73	7.218	0.8	0.385	0.8	0.91	0.136	0.3	2098	14
Z27	0.02	26	12	13	0.51	7.247	1.0	0.386	0.8	0.72	0.136	0.7	2103	14
Z28	0.02	25	11	9	0.37	6.937	1.2	0.372	1.0	0.80	0.135	0.7	2039	17
Z29	0.01	45	21	20	0.45	7.007	1.0	0.377	0.9	0.84	0.135	0.5	2060	16
Z30	0.03	14	6	5	0.36	7.128	2.3	0.385	1.7	0.73	0.134	1.6	2100	31

$f_{\text{206}}$ : the percentage of the common Pb found in  $^{206}\text{Pb}$ ; #: ratios corrected for common Pb; \*: zircons excluded from the calculation of age; \*\*: data used for concordant age calculation. Th/U ratios and amount of Pb, Th and U (in ppm) are calculated relative to Gf-1 reference zircon. Conc.: degree of concordance =  $(^{206}\text{Pb}/^{238}\text{U} \text{ age} / ^{207}\text{Pb}/^{235}\text{U} \text{ age}) * 100$ . Rho is the error correlation defined as the quotient of the propagated errors of the  $^{206}\text{Pb}/^{238}\text{U}$  and the  $^{207}\text{Pb}/^{235}\text{U}$  ratio.

Table 4. Summary of U-Pb zircon in situ data from sample obtained by LA-MC-ICP-MS from metatonalite (SR-05) of the Rosário suite.

Zircon	f <sub>206</sub> Spot (%)	U (ppm)	Pb (ppm)	Th (ppm)	Th/U (ppm)	207Pb/235U (%)	1s (%)	Ratios #		Ages (Ma)	
								206Pb/238U (%)	Rho	207Pb/206Pb (%)	1s (%)
Z1	0.01	45	23	30	0.68	7.230	0.9	0.389	0.8	0.83	0.5
Z2	0.01	34	17	21	0.62	7.359	1.0	0.395	0.8	0.81	0.6
Z3	0.01	29	14	16	0.54	7.169	0.9	0.387	0.7	0.76	0.5
Z4	0.02	29	13	19	0.65	7.161	1.1	0.385	0.8	0.73	0.7
Z5 *	0.02	25	12	17	0.68	7.454	1.2	0.397	1.0	0.81	0.7
Z6 *	0.01	40	19	23	0.57	7.412	1.2	0.396	1.0	0.83	0.6
Z7 *	0.01	43	19	17	0.40	7.499	0.8	0.399	0.7	0.80	0.5
Z8	0.01	71	37	29	0.41	7.202	0.8	0.386	0.8	0.91	0.3
Z9	0.02	33	19	15	0.47	7.275	1.4	0.388	1.3	0.94	0.4
Z10	0.02	21	11	8	0.41	7.033	1.3	0.375	1.1	0.87	0.6
Z11	0.02	12	7	5	0.41	6.861	2.0	0.361	1.6	0.81	0.3
Z12	0.03	15	8	6	0.40	6.877	1.8	0.365	1.3	0.71	0.4
Z13 *	0.01	30	17	17	0.57	7.428	1.0	0.398	0.7	0.71	0.7
Z14	0.01	51	17	15	0.50	7.222	1.1	0.388	0.9	0.79	0.7
Z15 *	0.01	41	22	23	0.57	7.521	0.9	0.402	0.7	0.80	0.5
Z16 *	0.01	64	35	41	0.65	7.517	1.1	0.400	0.8	0.73	0.7
Z17 *	0.01	45	25	20	0.45	7.455	1.3	0.401	1.0	0.82	0.7
Z18	0.01	34	22	17	0.51	7.820	1.4	0.421	1.0	0.73	0.9
Z19	0.02	27	15	11	0.42	7.623	1.2	0.407	1.0	0.87	0.5
Z20	0.02	24	14	11	0.45	7.329	1.3	0.386	1.0	0.76	0.8
Z21	0.02	57	32	37	0.66	7.061	0.9	0.378	0.7	0.72	0.6
Z22	0.01	43	24	26	0.62	7.521	0.9	0.390	0.8	0.82	0.5
Z23	0.01	63	33	27	0.44	7.367	1.1	0.394	1.0	0.89	0.5
Z24	0.01	52	27	34	0.66	7.086	0.9	0.381	0.7	0.75	0.5
Z25	0.02	32	19	15	0.46	7.067	1.3	0.374	1.0	0.76	0.8
Z26	0.04	11	6	0.50	6.990	2.5	0.371	1.9	0.76	0.137	1.6
Z27	0.04	18	10	11	0.65	7.039	2.0	0.372	1.4	0.72	0.137
Z28	0.03	18	10	11	0.63	6.975	1.5	0.371	1.2	0.81	0.136
Z29	0.03	20	11	7	0.35	7.082	1.5	0.381	1.2	0.80	0.135

f<sub>206</sub>: the percentage of the common Pb found in <sup>206</sup>Pb; #: ratios corrected for common Pb; \*data used for concordant age calculation.

Rho is the error correlation defined as the quotient of the propagated errors of the <sup>206</sup>Pb/238U and the <sup>207</sup>Pb/235U ratio.

Table 5. Summary of U-Pb zircon in situ data from sample obtained by LA-MC-ICP-MS from metatonalite (SR-06) of the Rosário suite.

Zircon	$f_{\text{206}}$ (%)	U (ppm)	Pb (ppm)	Th (ppm)	Th/U (ppm)	$^{207}\text{Pb}/^{235}\text{U}$	1s (%)	$^{206}\text{Pb}/^{238}\text{U}$ (%)	1s Rho	$^{207}\text{Pb}/^{206}\text{Pb}$	Ratios #		Ages (Ma)						
											1s (%)	$^{206}\text{Pb}/^{238}\text{U}$ (%)	1s (abs)	$^{207}\text{Pb}/^{206}\text{Pb}$ (abs)					
Z1	0.02	17.0	9.4	8.5	0.50	6.638	1.4	0.354	1.1	0.73	0.136	1.0	1956	18	2064	13	2175	17	95
Z2	0.02	23.8	13.5	16.0	0.68	6.731	1.3	0.355	1.1	0.80	0.137	0.8	1961	18	2077	12	2194	14	94
Z3	0.04	13.8	7.4	7.8	0.57	6.921	2.1	0.366	1.6	0.76	0.137	1.5	2011	27	2101	18	2191	24	96
Z4	0.03	11.7	7.4	8.5	0.73	6.763	1.6	0.355	1.2	0.77	0.138	1.0	1957	21	2081	14	2206	18	94
Z5	0.02	29.7	17.0	19.2	0.65	6.923	1.1	0.370	0.9	0.79	0.136	0.6	2029	15	2102	10	2174	11	97
Z6	0.02	23.1	13.5	11.9	0.52	7.062	1.1	0.373	0.9	0.79	0.137	0.6	2042	15	2119	9	2195	11	96
Z7	0.01	30.5	15.4	11.5	0.38	6.669	1.1	0.358	0.9	0.77	0.135	0.7	1973	15	2069	10	2165	13	95
Z8	0.03	13.6	7.8	4.6	0.34	6.709	2.0	0.353	1.6	0.78	0.138	1.5	1950	27	2074	18	2199	23	94
Z9	0.04	17.6	10.2	9.4	0.53	6.804	1.4	0.364	1.1	0.77	0.136	0.9	2000	19	2086	13	2172	16	96
Z11	0.02	9.9	6.2	5.3	0.53	6.873	1.1	0.365	0.8	0.75	0.136	0.7	2008	14	2095	10	2182	12	96
Z12	0.02	24.0	14.5	13.5	0.56	6.556	1.0	0.353	0.8	0.83	0.135	0.5	1951	14	2053	9	2158	9	95
Z13	0.02	52.4	27.9	26.9	0.52	7.085	1.3	0.381	1.0	0.76	0.135	0.8	2081	17	2122	11	2162	14	98
Z14	0.01	30.7	17.4	23.5	0.77	7.027	1.0	0.376	0.8	0.83	0.135	0.5	2059	14	2115	8	2170	9	97
Z15	0.01	41.4	22.6	16.6	0.40	7.566	0.9	0.408	0.8	0.83	0.134	0.5	2206	14	2181	8	2157	8	101
Z16	0.01	66.5	37.3	48.2	0.73	7.048	1.0	0.381	0.9	0.87	0.134	0.5	2080	16	2118	9	2154	8	98
Z17	0.02	34.1	18.5	13.1	0.39	7.037	1.2	0.379	1.0	0.87	0.135	0.6	2070	18	2116	10	2161	10	98
Z18	0.01	29.9	16.9	13.1	0.44	7.064	1.0	0.383	0.8	0.79	0.134	0.6	2089	14	2120	9	2149	11	99
Z19	0.03	19.3	11.3	11.0	0.58	7.116	1.3	0.383	1.0	0.74	0.135	0.8	2090	17	2126	11	2161	15	98
Z21	0.02	30.9	18.6	27.4	0.90	7.022	1.3	0.382	1.0	0.78	0.133	0.8	2084	19	2114	12	2144	14	99
Z22	0.04	11.3	6.7	5.8	0.52	7.165	2.4	0.381	1.8	0.74	0.136	1.6	2082	31	2132	21	2181	29	98
Z24	0.03	13.4	7.1	7.1	0.53	7.272	1.7	0.383	1.2	0.72	0.138	1.2	2089	22	2145	15	2199	21	97
Z26	0.02	16.9	8.9	8.3	0.49	7.103	1.9	0.376	1.3	0.68	0.137	1.4	2059	24	2124	17	2189	25	97
Z28	0.02	15.8	9.9	7.6	0.48	6.885	1.7	0.366	1.3	0.76	0.136	1.1	2010	23	2097	15	2183	20	96
Z27	0.01	39.5	23.2	27.8	0.71	7.035	1.1	0.377	0.9	0.85	0.135	0.5	2061	16	2116	9	2170	10	97
Z29	0.01	38.2	20.7	19.4	0.51	6.668	1.2	0.352	1.1	0.90	0.137	0.5	1945	19	2068	11	2193	9	94

$f_{\text{206}}$ : the percentage of the common Pb found in  $^{206}\text{Pb}$ ; #: ratios corrected for common Pb; Th/U ratios and amount of Pb, Th and U (in ppm) are calculated relative to Gl-1 reference zircon.  
 Rho is the error correlation defined as the quotient of the propagated errors of the  $^{206}\text{Pb}/^{238}\text{U}$  and the  $^{207}\text{Pb}/^{235}\text{U}$  ratio. Conc.: degree of concordance =  $(^{206}\text{Pb}/^{238}\text{U} \text{ age} / ^{207}\text{Pb}/^{235}\text{U} \text{ age}) * 100$ .

Table 6. Summary of U-Pb zircon in situ data from sample obtained by LA-MC-ICP-MS from Metatonalite (SR-09) of the Rosário suite.

Zircon	$f_{\text{206}}^*$ (%)	U (ppm)	Pb (ppm)	Th (ppm)	Th/U	$^{207}\text{Pb}/^{235}\text{U}$ (%)	1s	$^{206}\text{Pb}/^{238}\text{U}$ (%)	1s	Rho	$^{207}\text{Pb}/^{206}\text{Pb}$	1s	$^{206}\text{Pb}/^{238}\text{U}$ (%)	1s	$^{207}\text{Pb}/^{235}\text{U}$ (%)	1s	$^{207}\text{Pb}/^{206}\text{Pb}$ (abs)	1s	$^{207}\text{Pb}/^{235}\text{U}$ (abs)	1s	Conc. (%)			
							Ratios #				Ages (Ma)													
Z1	0.02	33.2	17.7	13.4	0.40	7.174	1.0	0.386	0.8	0.74	0.135	0.6	2105	14	2133	9	2160	12	99					
Z2	0.01	39.9	20.0	14.7	0.37	7.044	1.2	0.379	0.9	0.70	0.135	0.8	2074	15	2117	11	2159	15	98					
Z3	0.03	13.2	7.4	7.3	0.55	7.060	1.8	0.379	1.4	0.76	0.135	1.2	2070	25	2119	16	2167	21	98					
Z4	0.03	15.6	8.4	10.4	0.67	7.156	1.6	0.389	1.2	0.73	0.133	1.1	2120	21	2131	14	2142	19	99					
Z5	0.02	28.6	16.5	17.5	0.61	7.181	1.1	0.391	0.9	0.79	0.133	0.7	2127	17	2134	10	2141	12	100					
Z6	0.01	40.7	20.4	15.5	0.38	6.930	1.0	0.370	0.8	0.83	0.136	0.5	2031	15	2102	9	2173	10	97					
Z7	0.02	26.4	14.8	11.1	0.42	6.874	1.4	0.368	1.1	0.78	0.135	0.9	2020	20	2095	13	2170	16	96					
Z8	0.01	64.0	33.7	24.6	0.39	6.666	0.9	0.360	0.8	0.81	0.134	0.5	1981	13	2068	8	2156	9	96					
Z9	0.01	34.6	19.3	19.9	0.58	7.053	0.9	0.377	0.8	0.83	0.136	0.5	2062	14	2118	8	2173	9	97					
Z11	0.01	86.1	46.3	67.3	0.79	7.056	0.8	0.377	0.7	0.78	0.136	0.5	2062	12	2119	8	2174	9	97					
Z12	0.03	31.9	17.6	14.0	0.44	6.801	1.3	0.364	0.9	0.63	0.135	1.0	2003	15	2086	11	2169	18	96					
Z13	0.01	68.4	36.1	28.3	0.42	7.291	0.8	0.392	0.7	0.85	0.135	0.4	2134	13	2148	7	2161	7	99					
Z14	0.05	17.2	10.0	7.1	0.41	7.141	2.3	0.389	1.8	0.79	0.133	1.4	2118	33	2129	20	2140	25	99					
Z15	0.02	48.9	27.9	25.4	0.52	7.519	1.0	0.406	0.9	0.89	0.134	0.5	2196	17	2175	9	2156	8	101					
Z16	0.01	79.4	41.9	35.4	0.45	6.989	0.9	0.375	0.8	0.87	0.135	0.4	2054	15	2110	8	2165	8	97					
Z17	0.02	45.0	26.3	26.5	0.59	7.182	1.0	0.387	0.8	0.78	0.135	0.6	2108	14	2134	9	2159	10	99					
Z18	0.02	23.3	13.3	10.8	0.47	7.016	1.1	0.380	0.8	0.73	0.134	0.7	2075	14	2113	10	2151	13	98					
Z19	0.03	27.4	15.2	11.6	0.45	7.197	0.9	0.387	0.7	0.78	0.135	0.5	2107	13	2136	8	2164	10	99					
Z20	0.01	47.0	26.3	27.7	0.59	7.556	0.9	0.406	0.8	0.85	0.135	0.5	2198	15	2180	8	2162	8	101					
Z21	0.02	34.3	18.3	11.0	0.32	7.473	1.1	0.405	0.9	0.80	0.134	0.6	2191	16	2170	9	2150	11	101					
Z22	0.01	51.8	28.2	21.1	0.41	6.977	0.8	0.375	0.7	0.80	0.135	0.4	2055	12	2108	7	2161	8	97					
Z23 *	0.09	21.2	12.4	12.8	0.61	6.751	2.4	0.355	1.8	0.72	0.138	1.7	1961	30	2079	21	2199	30	94					
Z24	0.02	36.1	20.5	21.9	0.61	5.958	1.1	0.333	0.9	0.80	0.130	0.6	1853	14	1970	10	2094	11	94					
Z25	0.02	29.6	18.3	16.1	0.55	5.384	1.2	0.308	0.9	0.76	0.127	0.7	1729	14	1882	10	2056	14	92					
Z26	0.03	24.3	13.9	12.4	0.51	5.005	1.3	0.293	1.0	0.75	0.124	0.8	1655	14	1820	11	2014	15	91					
Z27	0.01	159.6	74.7	73.2	0.46	4.485	1.4	0.269	1.2	0.84	0.121	0.7	1534	16	1728	12	1973	14	89					
Z28 *	0.01	39.6	22.6	20.2	0.52	4.387	1.3	0.270	1.0	0.76	0.118	0.8	1539	14	1710	11	1926	15	90					
Z29	0.01	34.3	19.6	19.0	0.56	3.930	1.5	0.244	1.1	0.68	0.117	1.1	1409	14	1620	12	1906	20	87					

$f_{\text{206}}^*$ : the percentage of the common Pb found in  $^{206}\text{Pb}$ ; #: ratios corrected for common Pb; \*zircons excluded from the calculation of age.

Th/U ratios and amount of Pb, Th and U (in ppm) are calculated relative to GJ-1 reference zircon. Conc.: Degree of concordance =  $(^{206}\text{Pb}/^{238}\text{U} \text{ age} / ^{207}\text{Pb}/^{235}\text{U} \text{ age}) * 100$ .

Rho is the error correlation defined as the quotient of the propagated errors of the  $^{206}\text{Pb}/^{238}\text{U}$  and the  $^{207}\text{Pb}/^{235}\text{U}$  ratio.

Table 7. Summary of U-Pb zircon in situ data from sample obtained by LA-MC-ICP-MS from metagranodiorite (SR-08) of the Rosário suite.

Zircon	$f_{\text{206}}$	U	Pb	Th	Th/U	$^{207}\text{Pb}/^{235}\text{U}$	1s	$^{206}\text{Pb}/^{238}\text{U}$	1s	Rho	$^{207}\text{Pb}/^{206}\text{Pb}$	1s	$^{206}\text{Pb}/^{238}\text{U}$	1s	$^{207}\text{Pb}/^{235}\text{U}$	1s	$^{207}\text{Pb}/^{206}\text{Pb}$	1s	Conc.
Z01 *	0.76	352	100	151	0.45	2.007	1.5	0.152	1.5	0.92	0.096	0.6	914	11	1118	10	1540	11	82
Z03	0.05	298	75	107	0.36	1.337	1.5	0.098	1.2	0.80	0.099	0.9	603	7	862	9	1602	17	70
Z04 *	0.54	130	47	45	0.35	3.562	1.9	0.213	1.7	0.89	0.121	0.9	1246	19	1541	15	1973	16	81
Z05	0.01	90	39	24	0.27	5.442	2.1	0.299	1.9	0.88	0.132	1.0	1685	28	1892	18	2127	18	89
Z06 *	0.56	127	52	44	0.35	3.766	2.4	0.218	1.8	0.79	0.125	1.5	1272	21	1586	19	2032	26	80
Z07	0.00	174	83	48	0.28	6.991	1.3	0.374	1.1	0.88	0.135	0.6	2050	20	2110	11	2170	10	97
Z08	0.74	447	144	281	0.63	3.115	1.6	0.185	1.4	0.89	0.122	0.8	1095	14	1436	12	1986	14	76
Z10	0.01	145	71	50	0.35	7.581	1.2	0.406	1.0	0.78	0.135	0.7	2196	18	2183	11	2170	13	101
Z11	0.01	59	31	13	0.23	7.020	1.3	0.376	0.9	0.62	0.135	1.0	2060	15	2114	12	2167	18	97
Z12	0.01	140	73	44	0.32	7.673	1.2	0.409	1.0	0.86	0.136	0.6	2211	19	2193	10	2177	10	101
Z13	0.01	167	83	43	0.26	7.096	1.0	0.377	0.8	0.75	0.136	0.6	2063	14	2124	9	2183	11	97
Z14	0.01	215	91	66	0.31	6.309	1.0	0.342	0.8	0.82	0.134	0.5	1894	14	2020	9	2150	10	94
Z15 *	1.07	387	151	215	0.56	2.494	3.3	0.164	3.1	0.95	0.111	1.1	977	28	1270	24	1808	20	77
Z17	0.18	298	120	137	0.46	5.589	1.2	0.311	0.9	0.76	0.130	0.8	1747	14	1914	10	2101	14	91
Z18	0.01	210	71	85	0.41	7.052	1.1	0.375	1.0	0.82	0.136	0.6	2053	17	2118	10	2182	11	97
Z19 *	0.02	138	63	147	1.07	3.963	3.0	0.220	2.9	0.98	0.130	0.6	1283	34	1627	24	2105	11	79
Z20	0.01	222	82	65	0.29	6.996	1.5	0.372	1.4	0.93	0.136	0.5	2038	24	2111	13	2183	10	97
Z21	0.01	118	52	29	0.25	6.258	0.8	0.340	0.6	0.72	0.133	0.5	1888	10	2013	7	2143	10	94
Z22	0.06	257	99	91	0.36	5.977	1.2	0.328	1.0	0.85	0.132	0.6	1828	16	1973	10	2128	11	93
Z24	0.01	72	37	25	0.35	6.683	1.5	0.362	1.0	0.66	0.134	1.1	1992	18	2070	13	2149	20	96
Z25	0.03	46	21	19	0.42	6.346	2.1	0.343	1.6	0.74	0.134	1.4	1899	26	2025	18	2155	25	94
Z26	0.03	29	15	8	0.29	6.672	2.1	0.355	1.4	0.66	0.136	1.6	1960	24	2069	19	2179	28	95
Z27 *	0.00	21	10	7	0.34	6.564	2.5	0.368	1.6	0.62	0.129	1.9	2020	27	2055	22	2089	35	98

$f_{\text{206}}$ : the percentage of the common Pb found in  $^{206}\text{Pb}$ ; # : ratios corrected for common Pb; \*zircons excluded from the calculation of age. Th/U ratios and amount of Pb, Th and U (in ppm) are calculated relative to Gf-1 reference zircon. Conc: degree of concordance =  $(^{206}\text{Pb}/^{238}\text{U} \text{ age} / ^{207}\text{Pb}/^{235}\text{U} \text{ age})^*100$ . Rho is the error correlation defined as the quotient of the propagated errors of the  $^{206}\text{Pb}/^{238}\text{U}$  and the  $^{207}\text{Pb}/^{235}\text{U}$  ratio.

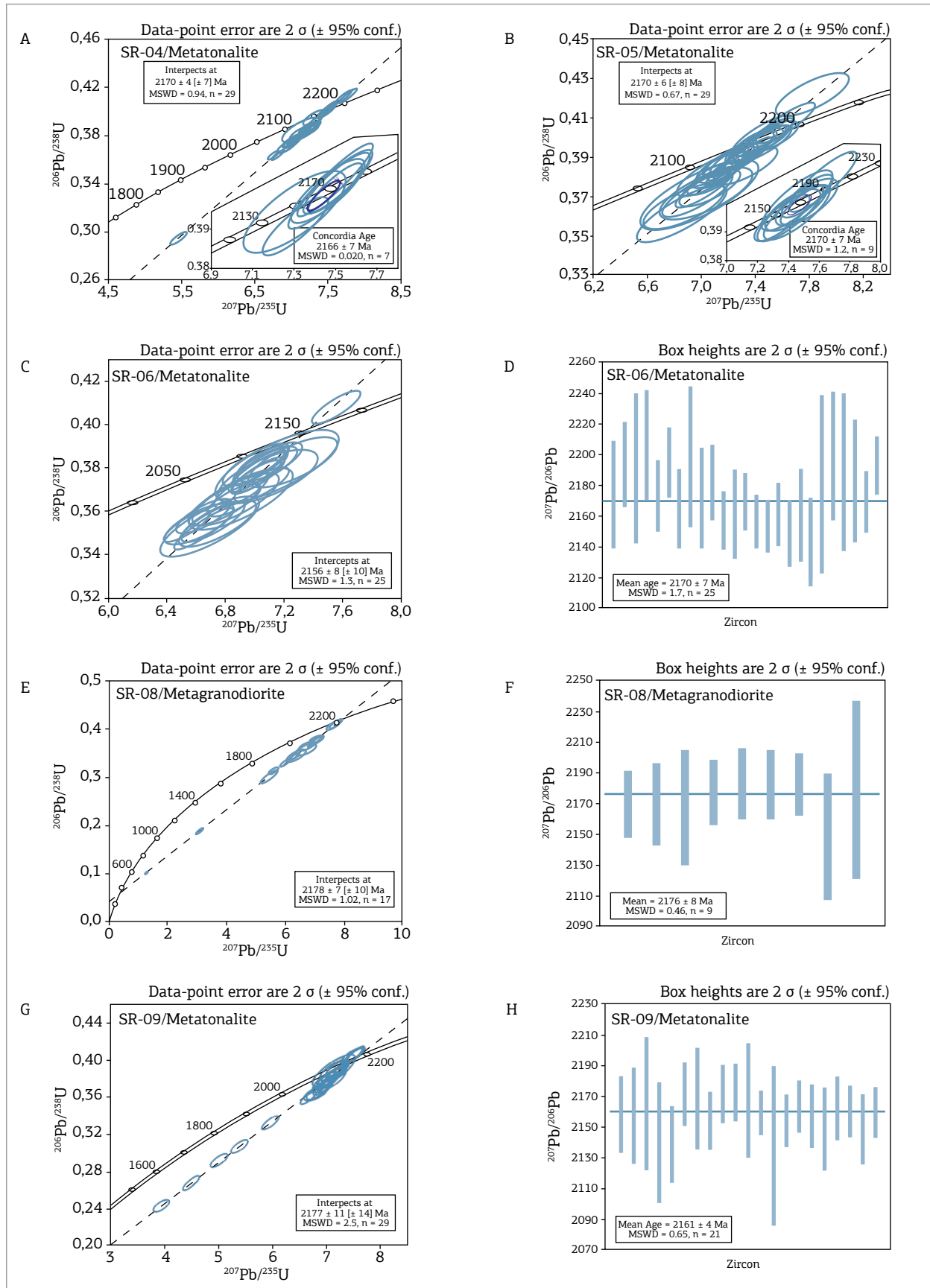


Figure 14.  $^{207}\text{Pb}/^{235}\text{U}$  versus  $^{206}\text{Pb}/^{238}\text{U}$  Concordia diagrams and weighted mean  $^{207}\text{Pb}/^{206}\text{Pb}$  age diagrams for the zircon grains analyzed by LA-ICP-MS.

Table 8. Whole-rock Sm-Nd isotopic data of metatonalite from Rosário Suite.

Sample	Sm (ppm)	Nd (ppm)	$^{147}\text{Sm}/^{144}\text{Nd}$	$2s$	$^{143}\text{Nd}/^{144}\text{Nd}$	$2s$	$f_{(\text{Sm/Nd})}$	$T_{(\text{DM})}$	$\varepsilon_{\text{Nd}}(2.2)$
SR-01	4.50	23.60	0.11521	0.00024	0.511621	0.000010	-0.41	2.21	+3.22
SR-02	3.80	19.95	0.11524	0.00013	0.511555	0.000007	-0.41	2.31	+1.91
SR-04	3.62	16.68	0.13138	0.00015	0.511825	0.000007	-0.33	2.26	+2.62
SR-09	4.36	21.88	0.12040	0.00043	0.511657	0.000027	-0.39	2.27	+2.45

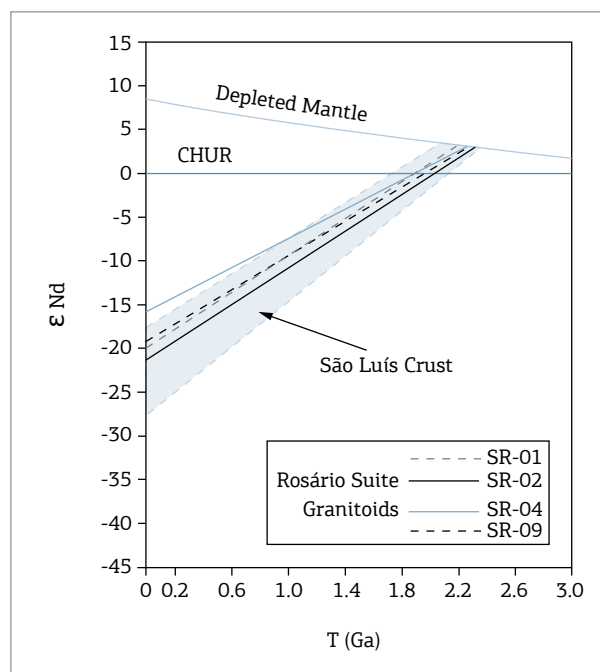


Figure 15.  $\varepsilon_{\text{Nd}}$  versus time diagram, showing the isotopic composition of the Rosário Suite. The field of the Paleoproterozoic São Luís crust is from Klein *et al.* (2005a, 2012).

## CONCLUSIONS

The geochemical characteristics combined with the field, petrographic, geochronological and isotopic data indicate that studied rocks are co-genetic and that compositional variations are associated with magmatic fractionation process. The different petrographic-compositional types possibly represent successions of magmatic pulses in an arc-related environment, but the samples dated here are essentially coeval. All five samples analyzed have yielded consistent U-Pb zircon ages with preferred results of  $2165 \pm 7$  Ma,  $2170 \pm 7$  Ma,  $2170 \pm 7$  Ma, for metatonalite and  $2161 \pm 4$  Ma for metagranodiorite, and  $2175 \pm 8$  Ma for metagranodiorite. Allowing for the inherent calibration uncertainty, these data suggest that the Rosário Suite plutonic rocks

were emplaced during a single magmatic episode between 2155 and 2175 Ma. These ages are slightly older than previous results of 2.08 to 2.13 Ga presented by Gorayeb *et al.* (1999) using the Pb zircon evaporation method. Younger ages are commonly expected by Pb evaporation method, providing minimum ages.

Our data show that emplacement of the Rosário Suite between about 2.15 and 2.18 Ma represents an important event of Paleoproterozoic crust formation during the Rhyacian period. Whole-rock Sm-Nd isotopic study provided  $T_{\text{DM}}$  model ages between 2.21 and 2.37 Ga, with low positive  $\varepsilon_{\text{Nd}}$  values, indicating that the Rosário Suite magmas had a short time of crustal residence, which implies an essentially juvenile nature.

The area where the Rosário Suite is located represents the most eastern exposures of the São Luís Craton, which are part of a large batholith of felsic to intermediate composition (diorites, tonalites, granodiorites, granites, leucogranites and andesites). Multiple plutons are probably involved, but it is not possible to delimit them on the scale of the mapping that has been carried out.

Geochemical data have demonstrated systematic variation in the major, minor and trace elements. In geochemical diagrams, all granitoids show trends of magmatic differentiation compatible to arc-related environment of the calc-alkaline series. They are metaluminous, calc-alkaline, I-type granitoids related to subduction environment of the continental magmatic arcs.

The structural data indicate the deformational effects of a regional transcurrent tectonic system, probably at more advanced stages of the Paleoproterozoic Transamazonian orogeny or subsequent Neoproterozoic tectonics of the Brasilian/Pan-African cycle that produced new structural features, such as mylonitic fabrics with comminution, rotation and overlapping processes of feldspars, biotite and hornblende. This tectonic condition also imposed different grades of stretching, recrystallization of quartz, saussuritization of plagioclase and neoformation of tremolite-actinolite and chlorite. The metamorphic conditions reached the greenschist facies. The deformation and metamorphic transformations are related to the collisional tectonic Transamazonian orogenesis in the Rhyacian period in other regions of the São Luís and Amazonian cratons.

The Rosário Suite is part of an extensive Rhyacian continental juvenile magmatic arc which is found in other parts of the São Luís Craton, which in the literature has been considered a fragment of the West African Craton. In Brazil, it is possible to correlate with the northwestern part of the Amazonian Craton, in which Rhyacian accretional magmatic arcs were amalgamated to form Archean terrains, more specifically in the northwest of the Pará state and Amapá. The Paleoproterozoic evolution of these cratons (2.24–2.1 Ga) is related to the Transamazonian orogenies, and the Rosário granitoids may represent the main accretion phase in the arc magmatic evolution.

## ACKNOWLEDGMENTS

We thank the Coordenação de Aperfeiçoamento de Pessoal de Nível Superior (CAPES) for the grant of a scholarship to the first author, and the Programa Institutos Nacionais de Ciência e Tecnologia (INCT)/Instituto Nacional de Ciência e Tecnologia de Geociências da Amazônia (GEOCIAM) Project — Ministério da Ciência, Tecnologia

e Inovação (MCT)/Conselho Nacional de Desenvolvimento Científico e Tecnológico (CNPq)/Fundação Amazônia de Amparo a Estudos e Pesquisas do Pará (FAPESPA) (Proc. no. 573733/2008-2) for financial support. We further acknowledge the Programa de Pós-Graduação em Geologia e Geoquímica (PPGG) do Instituto de Geociências (IG) of Universidade Federal do Pará (UFPA).

We are also grateful to the Geochronology Laboratory of UnB and technicians Felipe Valença de Oliveira and Luciana Pereira for their attention and support in obtaining cathodoluminescence images acquired by electron microscopy, and U-Pb zircon geochronological analysis by LA-ICP-MS. We thank the Pará-Iso for Sm-Nd analysis, for help in the recalculation of geochronological date. We are grateful to the Microanalysis Laboratory of UFPA for the support in the preparation of mounts of zircon grains, especially to Professor PhD Claudio Nery Lamarão, technicians Ana Paula Correa and Joelma Lobo. Finally, we would like to thank the reviewers and associate editor PhD Robert Pankhurst for their criticisms, corrections and suggestions that led to the improvement of the work.

## REFERENCES

- Abouchami W., Boher M., Michard A., Albarède F. 1990. A major 2.1 Ga event of mafic magmatism in West Africa: an early stage of crustal accretion. *Journal of Geophysical Research*, 95:17605-17629.
- Abreu F.A.M., Villas R.N.N., Hasui Y. 1980. Esboço estratigráfico do Pré-Cambriano da região do Gurupi, estados do Pará e Maranhão. In: SBG, Congresso Brasileiro de Geologia, 31, Camboriú. Anais, v.2, p.645-669.
- Almeida F.F.M., Hasui Y., Brito Neves B.B. 1976. The upper Precambrian of South America. *Boletim Instituto de Geociências USP*, 7:45-80.
- Boher M., Abouchami W., Albarède F., Arndt N.T. 1992. Crustal growth in West Africa at 2.1 Ga. *Journal of Geophysical Research*, 97:345-369.
- Boynton W.V. 1984. Cosmochemistry of the rare-earth elements: meteorite studies. In: Henderson P. (Ed.). *Rare-earth elements geochemistry*. Amsterdam, Elsevier, p.63-114.
- Brito-Neves B.B., Santos E.J., Van Schmus W.R. 2000. Tectonic history of the Borborema Province. In: Cordani U.G. Milani. E.J., Thomaz Filho A., Campos D.A. (eds.), *Tectonic evolution of the South America*. 3<sup>rd</sup> International Geological Congress, p.151-182.
- Brown G.C., Thorpe R.S., Webb P.C. 1984. The geochemical characteristics of granitoids in contrasting arcs and comments on source magmas. *Journal of the Geological Society*, 141:413-426.
- Bühn B., Pimentel M.M., Matteini M., Dantas E.L. 2009. High spatial resolution analysis of Pb and U isotopes for geochronology by laser ablation multi-collector inductively coupled plasma spectrometry (LA-MC-ICP-MS). *Anais da Academia Brasileira de Ciências*, 81:99-114.
- Chemale Jr. F., Mallmann G., Bitencourt M.F., Kawashita K. 2012. Time constraints on magmatism along the Major Gercino Shear Zone, southern Brazil: Implications for West Gondwana reconstruction. *Gondwana Research*, 22(1):184-189.
- Costa J.L. 2000. Folha SA.23-V-C Castanhal, Programa Levantamentos Geológicos Básicos do Brasil, Programa Grande Carajás, Belém, CPRM, CD-ROM.
- Cordani U.G., Sato K., Teixeira W., Basei M.A.S., Kawashita K. 1979. Evolução tectônica da Amazônia com base nos dados geocronológicos: Actas. II Congresso Geológico Chileno, 137-148.
- Cordani U.G. & Brito Neves, B.B. 1982. The geologic evolution of South America during the Archaean and Early Proterozoic. *Revista Brasileira de Geociências*, 12(1-3):78-88.
- Cox K.G., Bell J.D., Pankhurst R.J. 1979. *The interpretation of igneous rocks*. London, George Allen & Unwin, 450p.
- DePaolo D.J. 1981. A neodymium and strontium isotopic study of the mesozoic calc-alkaline granitic batholiths of the Sierra Nevada and Peninsular Ranges, California. *Journal of Geophysical Research*, 86:10470-10488.
- Fettes D. & Desmons J. 2008. *Metamorphic Rocks: A Classification and Glossary of Terms*. Recommendations of the International Union of Geological Sciences Subcommission on the Systematics of Metamorphic Rocks. Cambridge, Cambridge University Press. p. 240-256.
- Gasquet D., Barbey P., Adou M., Pasquette J.L. 2003. Structure, Sr-Nd isotope geochemistry and zircon U-Pb geochronology of the granitoids of the Dabakala área (Côte d'Ivoire): evidence for a 2.3 Ga crustal growth event in the Paleoproterozoic of West Africa? *Precambrian Research*, 127:329-354.
- Gill R. 2010. *Igneous rocks and process: a practical guide*. London, Wiley-Blackwell. 428p.
- Gioia S.M.C.L. & Pimentel M.M. 2000. The Sm-Nd isotopic method in the geochronology laboratory of the University of Brasília. *Anais da Academia Brasileira de Ciências*, 72:220-245.

- Gorayeb P.S.S., Gaudette H.E., Moura C.A.V., Abreu F.A.M. 1999. Geologia e geocronologia da Suíte Rosário, nordeste do Brasil, e sua contextualização geotectônica. *Revista Brasileira de Geociências*, 29:571-578.
- Hirdes W., Davis D.W., Ludtke G., Konan G. 1996. Two generations of Birrimian (Paleoproterozoic) volcanic belts in northeastern Côte d'Ivoire (West Africa): consequences for the "Birimian controversy". *Precambrian Research*, 80:173-191.
- Hurley P.M., Almeida F.F.M., Melcher G.C., Cordani U.G., Rand J.R., Kawashita K., Vandoros P., Pinson W.H., Fairbairn H.W. 1967. Test of continental drift by comparison of radiometric ages. *Science*, 157:495-500.
- Irvine T.N., Baragar W.R.A. 1971. A guide to the chemical classification of the common volcanic rocks. *Canadian Journal of Earth Sciences*, 8:523-546.
- Jackson S.E., Pearson N.J., Griffin W.L., Belousova E.A. 2004. The application of laser ablation-inductively coupled plasma-mass spectrometry to in situ U-Pb zircon geochronology. *Chemical Geology*, 211:47-69.
- Klein E.L., Lopes E.C. 2011. Geologia e recursos minerais da Folha Centro Novo do Maranhão – SA.23-Y-B-I, Estados do Maranhão e Pará, escala 1:100.000 – Belém. CPRM, p.57-87. CD-ROM.
- Klein E.L., Luzardo R., Moura C.A.V., Armstrong R. 2008. Geochemistry and geochronology of Paleoproterozoic granitoid magmatism: further evidence on the crustal evolution of the São Luís Craton, Brazil. *Precambrian Research*, 165:221-242.
- Klein E.L., Luzardo R., Moura C.A.V., Lobato D.C., Brito R.S.C., Armstrong R. 2009. Geochronology, Nd isotopes and reconnaissance geochemistry of volcanic and metavolcanic rocks of the São Luís Craton, northern Brazil: implications for tectonic setting and crustal evolution. *Journal of South American Earth Sciences*, 27:129-145.
- Klein E.L., Moura C.A.V. 2001. Age constraints on granitoids and metavolcanic rocks of the São Luís Craton and Gurupi belt, northern Brazil: implications for lithostratigraphy and geological evolution. *International Geology Review*, 43:237-253.
- Klein E.L., Moura C.A. V. 2008. São Luís Craton and Gurupi Belt (Brazil): possible links with the West-African Craton and surrounding Pan-African belts. In: Pankhurst R.J., Trouw R.A.J., Neves B.B.B., Wit M.J. (Eds.). West Gondwana: pre-cenozoic correlations across the South Atlantic region. *Geological Society of London. Special Publication*, 294:137-151.
- Klein E.L., Moura C.A.V., Krymsky R. S., Griffin W. L. 2005a. The Gurupi belt in northern Brazil: lithostratigraphy, geochronology, and geodynamic evolution. *Precambrian Research*, 141:83-105.
- Klein, E.L., Moura, C.A.V., Pinheiro, B. L. S. 2005b. Paleoproterozoic crustal evolution of the São Luís Craton, Brazil: evidence from zircon geochronology and Sm-Nd isotopes. *Gondwana Research*, 8:177-186.
- Klein E.L., Rodrigues J.B., Lopes E.C.S., Soledade G.L. 2012. Diversity of Rhyacian granitoids in the basement of the Neoproterozoic-Early Cambrian Gurupi Belt, northern Brazil: geochemistry, U-Pb zircon geochronology, and Nd isotope constraints on the Paleoproterozoic magmatic and crustal evolution. *Precambrian Research*, 220-221:192-216.
- Klein E.L., Tassinari C.C.G., Vasconcelos P.M. 2014. U-Pb Shrimp and 40Ar/39Ar constraints on the timing of mineralization in the Paleoproterozoic Caxias orogenic gold deposit, São Luís cratonic fragment, Brazil. *Journal of Geology*, 44:277-288.
- La Roche H. 1980. A classification of volcanic and plutonic rocks using R1-R2 diagram and major element analyses – its relationships with current nomenclature. *Chemical Geology*, 29:183-210.
- Lameyre J., Bowden P. 1982. Plutonic rock type series: discrimination of various granitoid series and related rocks. *Journal of Volcanology and Geothermal Research*, 14:169-186.
- Le Maitre R.W. 2002. *A classification of igneous rocks and glossary of terms*. 2<sup>nd</sup> Edition, London, Cambridge University Press, 193p.
- Lesquer A., Beltrão J.F., Abreu F.A.M. 1984. Proterozoic links between northeastern Brazil and West Africa: a plate tectonic model based on gravity data. *Tectonophysics*, 110:9-26.
- Ludwig K.R. 2003. *User's Manual for Isoplot/Ex version 3.00 – A Geochronology Toolkit for Microsoft Excel*, No. 4. Berkeley Geochronological Center, Special Publication, 70 p.
- Lugmair G.W. & Marti K. 1978. Lunar initial  $^{143}\text{Nd}/^{144}\text{Nd}$ : Differential evolution of the lunar crust and mantle. *Earth and Planetary Science Letters*, 39:349-357.
- McBirney A.R., White C.M. (1982). The Cascade Province. In: Thorpe R. S. (Ed.), *Andesites. orogenic andesites and related rocks*. New York, John Wiley & Sons, p.115-136.
- Oliveira E.C., Lafon J.M., Gioia S.M.C.L., Pimentel M.M. 2008. Datação Sm-Nd em rocha total e granada do metamorfismo granulítico da região de Tartarugal Grande, Amapá Central. *Revista Brasileira de Geociências*, 38:114-127.
- Palheta E.S., Abreu F.A.M., Moura C.A.V. 2009. Granitoides proterozoicos como marcadores da evolução geotectônica da região nordeste do Pará – Brasil. *Revista Brasileira de Geociências*, 39:647-657.
- Passchier C.W. & Trouw R.A.J. 1996. *Micro-tectonics*. Berlin, Springer-Verlag. 289p.
- Pearce J.A., Harris N.B.W., Tindle A.G. 1984. Trace element discrimination diagrams for the tectonic interpretation of granitic rocks. *Journal of Petrology*, 25:956-983.
- Rodrigues T.L.N., Favilla C.A.C., Camozzato E., Verissimo L.S. 1994. *Programa Levantamentos Geológicos Básicos do Brasil*. Bacabal. Folha SB.23-X-A. Estado do Maranhão. Escala 1:250.000. Brasília, CPRM. 124p. il.
- Rollinson H.R. 1993. *Using geochemical data: evaluation, presentation, interpretation*. New York, Longman, 352p.
- Rosa-Costa L.T., Lafon J.M., Delor C. 2006. Zircon geochronology and Sm-Nd isotopic study: further constraints for the Archean and Paleoproterozoic geodynamical evolution of the southeastern Guiana Shield, north of Amazonian Craton, Brazil. *Gondwana Research*, 10:277-300.
- Russell W.A., Papanastassiou D.A., Tombrello T.A. 1978. Ca isotope fractionation on the earth and other solar system materials. *Geochimica et Cosmochimica Acta*, 42(8):1075-1090.
- Santos J.O.S., Hartmann L.A., Gaudette H.E., Groves D.I., McNaughton N.J., Fletcher I.R. 2000. A new understanding on the provinces of the Amazon Craton based on integration of field mapping and U-Pb and Sm-Nd geochronology. *Gondwana Research*, 3(4):453-488.
- Sato K., Tassinari C.C.G. 1997. Principais eventos de acreção continental no Cráton Amazônico baseados em idade modelo Sm-Nd, calculada em evoluções de estágio único e estágio duplo. In: M.L. Costa & R.S. Angélica, (Eds.), *Contribuição à Geologia da Amazônia*. Belém, SBG-NO, p.91-142.
- Shand S.J. 1950. *Eruptive rocks, their genesis, composition, classification and their relation to ore-deposits*. Thomas Murby, London, 488 p.
- Sousa C.S., Klein E.L., Vasquez M.L., Lopes E.C.S., Teixeira S.G., Oliveira J.K.M., Moura E.M., Leão M.H.B. 2012. Mapa geológico e recursos minerais do estado do Maranhão. In: Klein E.L. & Sousa C.S. (Orgs.) *Geologia e recursos minerais do estado do Maranhão*. SIG, Escala 1:750.000. Belém, CPRM. ([www.geobank.cprm.gov.br/pls/public/Projetos](http://www.geobank.cprm.gov.br/pls/public/Projetos)).

- Stacey J.S. & Kramers J.D. 1975. Approximation of terrestrial lead isotope evolution by a two-stage model. *Earth and Planetary Science Letters*, 26(2):207-221.
- Streckeisen A.L. 1976. To each plutonic rock its proper name. *Earth-Science Reviews*, 12:1-33.
- Tassinari C.C.G. & Macambira M.J.B. 1999. Geochronological Provinces of the Amazonian Craton. *Episodes*, 22(3):174-182.
- Tassinari C.C.G. & Macambira M.J.B. 2004. A Evolução Tectônica Do Cráton Amazônico. In: Mantesso-Neto V., Bartorelli A., Carneiro C.D.R., Brito Neves B.B. (eds.), *Geologia do Continente Sul-Americano: Evolução da Obra de Fernando Flávio Marques de Almeida*. São Paulo, p. 471-485.
- Tassinari C.G., Bettencourt J.S., Geraldes M.C., Macambira M.J.B., Lafon J.M. 2000. The Amazon craton. In: Cordani U., Milani E.J., Thomaz Filho A., Campos D.A. Tectonic evolution of South America. 31st International Geological Congress, 2000. Rio de Janeiro. Anais... p. 41-95.
- Thiéblemont D., Tégyey M. 1994. Une discrimination géochimique des roches différencierées témoin de la diversité d'origine et de situation tectonique des magmas calcio-alcalins. *Comptes Rendus de l'Académie des Sciences*, 319:87-94.
- Thompson R.N. 1982. British Tertiary volcanic province. *Scottish Journal of Geology*, 18:49-107.
- Thorpe R.S., Francis P.W., Hammill M., Baker C.W. 1982. The Andes. In: R. S. Thorpe (ed.). *Andesites, orogenic andesites and related rocks*. New York, John Wiley & Sons, p.188-205.
- Torquato J.R., Cordani U.G. 1981. Brazil-Africa geological links. *Earth Science Reviews*, 17:155-176.
- Vasquez M.L., Rosa-Costa L.T. 2008. *Geologia e recursos minerais do Estado do Pará*. Programa Geologia do Brasil (PGE). Integração, atualização e difusão de dados da geologia do Brasil. Mapas geológicos estaduais. Escala 1:1.000.000. CD-ROM.
- Wiedenbeck M., Alle P., Corfu F., Griffin W.L., Meier M., Oberli F., Von Quadt A., Roddick J.C., Spiegel W. 1995. Three natural zircon standards for U-Th-Pb, Lu-Hf, trace element and REE analyses. *Geostandards Newsletter*, 19(1):1-23.
- Wilson M. 1989. *Igneous petrogenesis - a global tectonic approach*. Unwin Hyman Ltd, London.
- Winter D. 2001. *An introduction to igneous and metamorphic petrology*. Prentice Hall, New Jersey. 796p.
- Wright J.B., Hastings D.A., Jones W.B., Williams H.R. 1995. *Geology and mineral resources of West Africa*. London, Allen & Unwin, 187p.

---

Available at [www.sbg.org.br](http://www.sbg.org.br)

---

#### Appendix A. List of studied samples with geographic coordinates.

SAMPLE	Latitude	Longitude	Rock
2013/SR-01	02°54'5.32"S	44°19'46.6"W	Metatonalite
2013/SR-02	02°53'43.7"S	44°18'59.8"W	Metatonalite
2013/SR-03	02°55'46.5"S	44°13'40.1"W	Metatonalite
2013/SR-04	02°54'34.5"S	44°13'58.8"W	Metatonalite
2013/SR-05	02°55'2.77"S	44°13'53.77"S	Metamelatalonalite
2013/SR-06	02°53'49.48"S	44°19'24.65"W	Metatonalite
2013/SR-07	02°52'52.24"S	44°16'2.70"W	Metagranodiorite
2013/SR-08	02°55'39.41"S	44°03'50.56"W	Metagranodiorite
2013/SR-09	02°52'57.20"S	44°18'11.02"W	Metatonalite
2013/SR-10	02°52'27.83"S	44°17'5.00"W	Metagranodiorite
1993/BR-12a	02°52'16.06"S	44°13'17.90"W	Metaquartz diorite
1993/BR-12b	02°52'16.06"S	44°13'17.90"W	Metatonalite
1993/BR-13	02°54'27.90"S	44°16'38.63"W	Metaquartz diorite
1993/BR-14a	02°54'55.22"S	44°18'11.28"W	Metagranodiorite
1993/BR-14b	02°54'55.22"S	44°18'11.28"W	Metaquartz diorite
1993/BR-15	02°54'26.72"S	44°19'2.355W	Metaquartz diorite